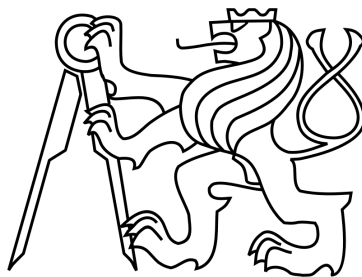


CZECH TECHNICAL UNIVERSITY IN PRAGUE
FACULTY OF CIVIL ENGINEERING
Department of Mechanics



DIPLOMA THESIS
Micromechanics-Based Models of
Cocciopesto Mortars

Václav Nežerka

2011

Supervisor: Jan Zeman

Honesty Declaration

I declare that this diploma thesis has been carried out by me and only with the use of materials that are stated in the literature sources.

December 05, 2011

Václav Nežerka

.....

Acknowledgement

I would like to thank my supervisor, Jan Zeman, who supported me, introduced me to the issues of micromechanics and explained me patiently everything I needed. I also want to thank to Professor Petr Kabele for his trust in me and for giving me the opportunity to be a member of his team and for his support.

Special thanks go to my friend Michael Somr for his willingness to discuss any problem I encountered during my entire study period and my parents for their continuous support and tolerance.

Finally, I would like to thank for the financial support by the grant no. DF11P01OVV008.



ČESKÉ VYSOKÉ UČENÍ TECHNICKÉ V PRAZE

Fakulta stavební

Thákurova 7, 166 29 Praha 6

ZADÁNÍ DIPLOMOVÉ PRÁCE

studijní program: Civil Engineering
studijní obor: Building Structures
akademický rok: 2011/2012

Jméno a příjmení diplomanta: Václav Nežerka

Zadávající katedra: K 132-Katedra mechaniky

Vedoucí diplomové práce: Doc. Ing. Jan Zeman, Ph.D.

Název diplomové práce: Micromechanics-based models of cocchiopesto mortars

Název diplomové práce
v anglickém jazyce: Micromechanics-based models of cocchiopesto mortars

Rámcový obsah diplomové práce: Studium literatury (chování malt na bázi cocchiopesto, základní mikromechanické modely pro odhad elastických vlastností a pevnosti)

Návrh, implementace a ověření mikromechanického modelu založeného na metodě Mori-Tanaka

Využití modelu pro predikci chování vybraných systémů, formulace výsledků analýzy.

Datum zadání diplomové práce: 14.9.2011 Termín odevzdání: 16.12.2011
(vyplňte poslední den výuky přísl. semestru)

Diplomovou práci lze zapsat, kromě oboru A, v letním i zimním semestru.

Pokud student neodevzdal diplomovou práci v určeném termínu, tuto skutečnost předem písemně zdůvodnil a omluva byla děkanem uznána, stanoví děkan studentovi náhradní termín odevzdání diplomové práce. Pokud se však student řádně neomluvil nebo omluva nebyla děkanem uznána, může si student zapsat diplomovou práci podruhé. Studentovi, který při opakovaném zápisu diplomovou práci neodevzdal v určeném termínu a tuto skutečnost řádně neomluvil nebo omluva nebyla děkanem uznána, se ukončuje studium podle § 56 zákona o VŠ č.111/1998 (SZŘ ČVUT čl 21, odst. 4).

Diplomant bere na vědomí, že je povinen vypracovat diplomovou práci samostatně, bez cizí pomoci, s výjimkou poskytnutých konzultací. Seznam použité literatury, jiných pramenů a jmen konzultantů je třeba uvést v diplomové práci.


vedoucí diplomové práce


vedoucí katedry

Zadání diplomové práce převzal dne: 14. 9. 2011


diplomant

Abstract

Lime-based mortars were used for a construction of historic buildings and the present conservation practice is using this type of mortars because of their compatibility with the original materials. The cocchiopesto mortars, containing pieces of crushed bricks (or other burnt clay products), were used mainly during the Byzantine and Roman period. These mortars exhibit quite extraordinary mechanical properties due to formation of C-S-H gel coating on the interface of lime and fragments of the crushed clay products.

The micromechanical approach and Mori-Tanaka homogenization of coated particles explain some specific features of cocchiopesto mortars. The calculations indicate trends for different composition of mortar, porosity and size of crushed brick particles. The special attention is paid mainly to the influence of crushed bricks within the mix on the effective elastic stiffness and strength. The suggested approach enables an optimization of the mortar composition towards a better performance.

Keywords: cocchiopesto, micromechanics, Mori-Tanaka, strength estimation, C-S-H coating

Abstrakt

Vápenné malty byly využívány pro konstrukci historických staveb a současná památková péče využívá tento typ malt kvůli jejich kompatibilitě s původními materiály. Malty typu cocchiopesto, obsahující kousky drcených cihel (nebo jiných pálených produktů z keramické hlíny), byly používány zejména během byzantského období a ve Starověkém Římě. Tyto malty se vyznačují výjimečnými mechanickými vlastnostmi díky formaci tenké vrstvy C-S-H gelu na povrchu drcených cihel.

Mikromechanický přístup a homogenizace technikou Mori-Tanaka, modifikovanou pro částice potažené tenkou vrstvou, vysvětlují některé specifické vlastnosti malt typu cocchiopesto. Výpočty naznačují trendy pro různé složení malty, porositu a velikost drcených cihel. Zvláštní pozornost je věnována zejména vlivu drcených cihel ve směsi na efektivní elastickou tuhost a pevnost. Navrhovaný přístup umožňuje optimalizaci směsi směrem k lepším mechanickým vlastnostem.

Klíčová slova: cocchiopesto, mikromechanika, Mori-Tanaka, odhad pevnosti, vrstva C-S-H

Contents

Introduction.....	8
Goals.....	9
PART I: THEORETICAL BACKGROUND	10
1 Elasticity Equations	11
1.1 Stress-to-Displacement Relations.....	11
1.1.1 Displacements.....	11
1.1.2 Strains	12
1.2 Static Equations	14
1.2.1 Principal Stress.....	15
1.3 Constitutive Relations.....	16
2 Hydrostatic and Deviatoric Components	20
2.1 Hydrostatic and Deviatoric Stresses.....	20
2.2 Hydrostatic and Deviatoric Strains.....	21
2.3 Constitutive Relations.....	22
2.3.1 Index Notation, Lamé's Constants	23
2.3.2 Tensorial Notation.....	25
2.3.3 Engineering Notation.....	27
3 Stiffness Homogenization	29
3.1 Eigenstrain	29
3.1.1 Inclusions.....	29
3.1.2 Eshelby's Solution.....	29
3.2 Inhomogeneities	31
3.3 Effective Elastic Properties	33
3.3.1 Averaging.....	33
3.3.2 Effective Elastic Constants	35
3.3.3 Voigt and Reuss Approximation.....	36
3.3.3.1 Voigt Approximation	36
3.3.3.2 Reuss Approximation.....	37
3.3.4 Dilute (Non-Interacting) Defect Distribution.....	37
3.3.5 Mori-Tanaka Model.....	38
4 Strength Homogenization.....	42
4.1 Quadratic Strain Averages	42
5 Homogenization with Coated Particles	45
5.1 Hydrostatic Part	46
5.2 Deviatoric Part.....	46
5.3 Modification of Mori-Tanaka Homogenization.....	48

PART II: CALCULATIONS	50
6 Introduction to Cocciopesto Mortars.....	51
7 Calculation without C-S-H Gel Coating.....	53
7.1 Calculation of Effective Stiffness without C-S-H Gel Formation.....	54
7.2 Estimation of Strength without C-S-H Gel Formation.....	55
8 Calculation with C-S-H Gel Coating.....	58
8.1 Calculation of Effective Stiffness with C-S-H Gel Formation.....	59
8.2 Estimation of Strength with C-S-H Gel Formation.....	61
9 Calculation with Multiple Brick Fractions.....	62
9.1 Crushed Brick Size Optimization.....	64
Conclusion.....	67
REFERENCES	68

Introduction

The present conservation practice uses air lime or hydraulic lime mortars, because these are compatible with the original materials. The use of air lime presents problems with slow setting, inability to harden under water, lack of durability and poor mechanical strength. Therefore, the hydraulic lime-pozzolan mortars were widely used in the past and are still used nowadays for repair. These mortars are of higher porosity and lower strength than cement-based mortars, but they exhibit better durability.

Phoenicians were probably the first ones who added crushed clay products, such as burnt bricks, tiles or pieces of pottery, to the lime mortar in order to increase its durability and strength. Romans used this type of mortar in areas where other natural pozzolans were not available and called such material "cocciopesto". The structures, mainly from the Byzantine period, have also very thick joints, often comparable to the size of bricks. Together with the enhanced mechanical properties of the cocciopesto mortar, the use of the thick joints probably results in the increased resistance to earthquake loading, since the non-linear behavior of the mortar allows for better energy dissipation.

By closer investigation, it was found that the mortars containing crushed clay products exhibit a hydraulic character due to formation of C-S-H gel on the lime-brick interface. This component is responsible for some extraordinary properties of portland cement concrete and also the positive features of the lime-crushed brick mortars can be attributed to the high strength and quite stiffness of the C-S-H gel coating.

The development of the micromechanical model was inspired by other works, such as [1], using similar techniques for an estimation of material properties of concrete or cement-based mortars. In particular, the Mori-Tanaka method, modified for the homogenization of coated particles, was chosen for the calculation of the effective mortar stiffness and strength estimation. Even though these models are not expected to provide exact values, they should be able to predict the trends and therefore provide an explanation for the characteristic properties of the mortars containing crushed clay products.

The first part of this work provides a theoretical background of the micromechanical homogenization. In particular, the governing equations of linear elasticity, decomposition of stress and strain tensors to volumetric and deviatoric parts, stiffness homogenization of uncoated and coated particles and strength estimation are briefly explained. In the second part, the reader is introduced to the issue of cocciopesto mortars and the influence of individual components, mortar porosity and size of crushed brick particles is investigated. All the calculations presented in this work were done using the MATLAB software.

Goals

The main goal of this diploma thesis is to investigate the behavior of historic cocciopesto mortars. In particular, the main goals of the thesis are to:

- study the issues of mortars with crushed bricks
- study the influence of the C-S-H gel formation on the brick-matrix interface
- study the homogenization techniques and their theoretical background
- study the techniques for strength estimation
- create a reliable program for homogenization and strength estimation
- decide the appropriate composition of investigated mortar
- investigate the influence of individual constituents and C-S-H gel formation on the effective mortar stiffness, with an emphasis on the influence of crushed bricks in the mix
- investigate the influence of individual constituents and C-S-H gel formation on the mortar strength
- interpret the results and explain of the specific behavior of cocciopesto mortars

PART I:
THEORETICAL
BACKGROUND

1 Elasticity Equations

The governing equations of elasticity involve displacement, strain and stress fields, and they are valid if the structure undergoes only small deformations and the material behaves in a linearly elastic manner. Scheme of the overall system appears summarized in Fig. 1.1.

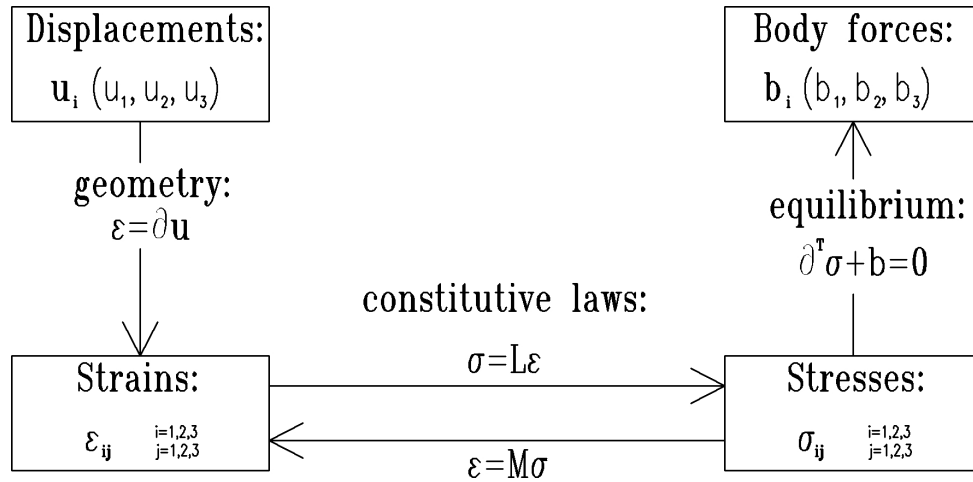


Fig. 1.1: Diagram of kinematic and static equations

1.1 Stress-to-Displacement Relations

1.1.1 Displacements

The displacements of the points within an elastic body are described by three components (u, v, w) or (u_1, u_2, u_3) , all of them dependent on the position in the Cartesian coordinate system (x, y, z) or (x_1, x_2, x_3) . In a matrix notation, the displacements are arranged in a vector as follows:

$$\mathbf{u}(\mathbf{x}) = \begin{Bmatrix} u_1(x_1, x_2, x_3) \\ u_2(x_1, x_2, x_3) \\ u_3(x_1, x_2, x_3) \end{Bmatrix} \quad (1.01)$$

while in the index notation, the field of displacements can be described as

$$u_i(x_j) \quad \begin{matrix} i = 1, 2, 3 \\ j = 1, 2, 3 \end{matrix} \quad (1.02)$$

1.1.2 Strains

Strains describe the deformation of the body. At a point, the stretching, e.g. in the x -direction, can be seen as the differential displacement per unit length. The x -component of strain is then

$$\varepsilon_x = \lim_{\Delta x \rightarrow 0} \frac{\Delta u(x, y, z)}{\Delta x} = \frac{\partial u}{\partial x} \quad (1.03)$$

therefore, the normal strain can be understood as a displacement gradient. The distortion of the material, which can be described as the change in originally right angles, is the sum of tilts imparted to vertical and horizontal lines (also called engineering strain):

$$\gamma_{xy} = \gamma_1 + \gamma_2 \approx \tan \gamma_1 + \tan \gamma_2 = \frac{\partial v}{\partial x} + \frac{\partial u}{\partial y} \quad (1.04)$$

For other displacement gradients ε_y , ε_z and distortions γ_{yz} , γ_{zx} the same reasoning can be applied with cyclic change of coordinates $x \rightarrow y \rightarrow z \rightarrow x$ and displacements $u \rightarrow v \rightarrow w \rightarrow u$.

The strain is a second order tensor and therefore the components can be arranged as follows:

$$\boldsymbol{\varepsilon} = \begin{bmatrix} \frac{\partial u}{\partial x} & \frac{1}{2} \left(\frac{\partial u}{\partial y} + \frac{\partial v}{\partial x} \right) & \frac{1}{2} \left(\frac{\partial u}{\partial z} + \frac{\partial w}{\partial x} \right) \\ \frac{1}{2} \left(\frac{\partial u}{\partial y} + \frac{\partial v}{\partial x} \right) & \frac{\partial v}{\partial y} & \frac{1}{2} \left(\frac{\partial v}{\partial z} + \frac{\partial w}{\partial y} \right) \\ \frac{1}{2} \left(\frac{\partial u}{\partial z} + \frac{\partial w}{\partial x} \right) & \frac{1}{2} \left(\frac{\partial v}{\partial z} + \frac{\partial w}{\partial y} \right) & \frac{\partial w}{\partial z} \end{bmatrix} \quad (1.05)$$

where, in the tensorial notation, shear strains (distortions) are halves of the engineering strains. The difference between vectors (first order tensors) and second order tensors shows up in how they transform with respect to coordinate rotations.

The index notation provides a compact description of all the components of three-dimensional states of strain:

$$\varepsilon_{ij} = \frac{1}{2} \left(\frac{\partial u_i}{\partial x_j} + \frac{\partial u_j}{\partial x_i} \right) = \frac{1}{2} (u_{i,j} + u_{j,i}) \quad (1.06)$$

where the comma denotes differentiation with respect to the following spatial variable (partial derivative). This double-subscript index notation leads naturally to a matrix arrangement of the strain components, in which the i - j component of the strain becomes the matrix element in the i^{th} row and the j^{th} column:

$$\boldsymbol{\varepsilon} = \begin{bmatrix} \varepsilon_{11} & \varepsilon_{12} & \varepsilon_{13} \\ \varepsilon_{21} & \varepsilon_{22} & \varepsilon_{23} \\ \varepsilon_{31} & \varepsilon_{32} & \varepsilon_{33} \end{bmatrix} = \begin{bmatrix} \frac{\partial u_1}{\partial x_1} & \frac{1}{2} \left(\frac{\partial u_1}{\partial x_2} + \frac{\partial u_2}{\partial x_1} \right) & \frac{1}{2} \left(\frac{\partial u_1}{\partial x_3} + \frac{\partial u_3}{\partial x_1} \right) \\ \frac{1}{2} \left(\frac{\partial u_1}{\partial x_2} + \frac{\partial u_2}{\partial x_1} \right) & \frac{\partial u_2}{\partial x_2} & \frac{1}{2} \left(\frac{\partial u_2}{\partial x_3} + \frac{\partial u_3}{\partial x_2} \right) \\ \frac{1}{2} \left(\frac{\partial u_1}{\partial x_3} + \frac{\partial u_3}{\partial x_1} \right) & \frac{1}{2} \left(\frac{\partial u_2}{\partial x_3} + \frac{\partial u_3}{\partial x_2} \right) & \frac{\partial u_3}{\partial x_3} \end{bmatrix} \quad (1.07)$$

Since the strain tensor is symmetric, i.e. $\varepsilon_{ij} = \varepsilon_{ji}$, there are six rather than nine independent strains, as might have been expected [2].

Sometimes it is convenient to arrange the strain components in a vector, or rather pseudovector. Strain is actually a 2nd order tensor, like stress or moment of inertia, and has mathematical properties very different from those of vectors, which must be taken into account while transforming or calculating the norm of strain. The ordering of the elements in the pseudovector is arbitrary, but it is conventional to list them in order (1, 1), (2, 2), (3, 3), (2, 3), (1, 3), (1, 2) [2]. This arrangement yields so-called Voigt notation.

Following the rules of a matrix multiplication, the strain pseudovector can also be written in terms of the displacement vector and proper operator. The strain-displacement relationship can be expressed as

$$\boldsymbol{\varepsilon} = \partial \mathbf{u} \quad (1.08)$$

$$\begin{Bmatrix} \varepsilon_x \\ \varepsilon_y \\ \varepsilon_z \\ \gamma_{yz} \\ \gamma_{xz} \\ \gamma_{xy} \end{Bmatrix} = \begin{bmatrix} \partial/\partial x & 0 & 0 \\ 0 & \partial/\partial y & 0 \\ 0 & 0 & \partial/\partial z \\ 0 & \partial/\partial z & \partial/\partial y \\ \partial/\partial z & 0 & \partial/\partial x \\ \partial/\partial y & \partial/\partial x & 0 \end{bmatrix} \begin{Bmatrix} u \\ v \\ w \end{Bmatrix}$$

In so-called Mandel notation, the components of strain are arranged in the pseudovector and the shear components of strain tensor are multiplied by $\sqrt{2}$ as follows:

$$\begin{Bmatrix} \varepsilon_{11} \\ \varepsilon_{22} \\ \varepsilon_{33} \\ \sqrt{2} \varepsilon_{23} \\ \sqrt{2} \varepsilon_{13} \\ \sqrt{2} \varepsilon_{12} \end{Bmatrix} = \begin{bmatrix} \partial/\partial x & 0 & 0 \\ 0 & \partial/\partial y & 0 \\ 0 & 0 & \partial/\partial z \\ 0 & (\sqrt{2}/2)(\partial/\partial z) & (\sqrt{2}/2)(\partial/\partial y) \\ (\sqrt{2}/2)(\partial/\partial z) & 0 & (\sqrt{2}/2)(\partial/\partial x) \\ (\sqrt{2}/2)(\partial/\partial y) & (\sqrt{2}/2)(\partial/\partial x) & 0 \end{bmatrix} \begin{Bmatrix} u \\ v \\ w \end{Bmatrix} \quad (1.09)$$

Such arrangement brings simplifications to many operations.

1.2 Static Equations

The force equilibrium on an infinitesimal cube results in the following equations (Cauchy's equations):

$$\begin{aligned}\frac{\partial \sigma_x}{\partial x} + \frac{\partial \tau_{yx}}{\partial y} + \frac{\partial \tau_{zx}}{\partial z} + b_x &= 0 \\ \frac{\partial \tau_{xy}}{\partial x} + \frac{\partial \sigma_y}{\partial y} + \frac{\partial \tau_{zy}}{\partial z} + b_y &= 0 \\ \frac{\partial \tau_{xz}}{\partial x} + \frac{\partial \tau_{yz}}{\partial y} + \frac{\partial \sigma_z}{\partial z} + b_z &= 0\end{aligned}\tag{1.10}$$

where b_i are body forces, such as gravity. These equations can be written using the index notation as

$$\sigma_{ij,j} + b_i = 0\tag{1.11}$$

In a pseudovector-matrix form we can write

$$\begin{bmatrix} \frac{\partial}{\partial x} & 0 & 0 & 0 & \frac{\partial}{\partial z} & \frac{\partial}{\partial y} \\ 0 & \frac{\partial}{\partial y} & 0 & \frac{\partial}{\partial z} & 0 & \frac{\partial}{\partial x} \\ 0 & 0 & \frac{\partial}{\partial z} & \frac{\partial}{\partial y} & \frac{\partial}{\partial x} & 0 \end{bmatrix} \begin{Bmatrix} \sigma_x \\ \sigma_y \\ \sigma_z \\ \tau_{yz} \\ \tau_{xz} \\ \tau_{xy} \end{Bmatrix} + \begin{Bmatrix} b_x \\ b_y \\ b_z \end{Bmatrix} = \begin{Bmatrix} 0 \\ 0 \\ 0 \end{Bmatrix}\tag{1.12}$$

From the moment equilibrium on the infinitesimal cube, we get:

$$\begin{aligned}\tau_{yz} &= \tau_{zy} \\ \tau_{zx} &= \tau_{xz} \\ \tau_{xy} &= \tau_{yx}\end{aligned}\tag{1.13}$$

due to this fact the stress tensor, here in the matrix representation,

$$\boldsymbol{\sigma} = \sigma_{ij} = \begin{bmatrix} \sigma_{11} & \sigma_{12} & \sigma_{13} \\ \sigma_{21} & \sigma_{22} & \sigma_{23} \\ \sigma_{31} & \sigma_{32} & \sigma_{33} \end{bmatrix}\tag{1.14}$$

is also symmetric. The element in the i^{th} row and the j^{th} column of this matrix is the stress on the i^{th} face in the j^{th} direction.

Equilibrium of the stress and surface traction on the boundary can be expressed by Cauchy's formula. It requests the equilibrium of the external traction forces with internal stress. The traction \mathbf{t} is associated with any plane with normal \mathbf{n} . It is a stress on the surface of the body

$$\mathbf{t} = \lim_{\Delta A \rightarrow 0} \frac{\Delta \mathbf{F}}{\Delta A} \quad (1.15)$$

where the externally applied force \mathbf{F} comprises of components in direction of coordinates. Therefore, the traction \mathbf{t} is completely defined by three traction vectors associated with coordinate planes, for instance

$$\mathbf{t}^{(x)} = \begin{Bmatrix} \sigma_x \\ \tau_{xy} \\ \tau_{xz} \end{Bmatrix} \quad (1.16)$$

generally, for an arbitrary normal plane \mathbf{n} it holds that

$$\mathbf{t}^{(n)} = \mathbf{t}^{(x)} n_x + \mathbf{t}^{(y)} n_y + \mathbf{t}^{(z)} n_z \quad (1.17)$$

which can be written in compact form as

$$\mathbf{t} = \boldsymbol{\sigma} \mathbf{n} \quad (1.18)$$

and in the index notation as

$$t_j^{(n)} = \sigma_{ij} n_i \quad (1.19)$$

where n_i is a multiple of the cosine angle between the investigated plane and coordinate system (it is a projection onto the coordinate axes).

1.2.1 Principal Stress

To find the stress on the plane where the corresponding traction vector is perpendicular to it and shear stresses vanish we put

$$\boldsymbol{\sigma} \mathbf{n} = \sigma \mathbf{n} \quad (1.20)$$

where the stress on the right hand side of the equation is so called principal stress. The equation can be expressed as

$$(\boldsymbol{\sigma} - \sigma \mathbf{I}) \mathbf{n} = 0 \quad (1.21)$$

where \mathbf{I} is the identity matrix. A non-trivial solution is obtained if

$$\det(\boldsymbol{\sigma} - \sigma \mathbf{I}) = 0 \quad (1.22)$$

Calculation of the determinant leads to the following characteristic equation:

$$\sigma^3 - I_1 \sigma^2 - I_2 \sigma - I_3 = 0 \quad (1.23)$$

where I_1, I_2, I_3 are so called invariants of the stress tensor (their values remain the same whatever the rotation of the coordinate system is). The first invariant is

$$I_1 = \sigma_x + \sigma_y + \sigma_z \quad (1.24)$$

the second one can be calculated as

$$I_2 = \det \begin{bmatrix} \sigma_y & \tau_{yz} \\ \tau_{zy} & \sigma_z \end{bmatrix} + \det \begin{bmatrix} \sigma_x & \tau_{xz} \\ \tau_{zx} & \sigma_z \end{bmatrix} + \det \begin{bmatrix} \sigma_x & \tau_{xy} \\ \tau_{yx} & \sigma_y \end{bmatrix} \quad (1.25)$$

Finally, the third stress invariant can be expressed as

$$I_3 = \det \begin{bmatrix} \sigma_x & \tau_{xy} & \tau_{xz} \\ \tau_{yx} & \sigma_y & \tau_{yz} \\ \tau_{zx} & \tau_{zy} & \sigma_z \end{bmatrix} \quad (1.26)$$

The same reasoning is used for calculation of the principal strain calculation and strain tensor invariants.

1.3 Constitutive Relations

The previous sections deal only with the kinematics (geometry) and static equilibrium of the body; however, they do not provide insight on the role of the material itself. The kinematic equations relate strains to displacement gradients, and the equilibrium equations relate stress to the applied tractions on loaded boundaries and also provide the relations among stress gradients within the material. Six more equations, relating the stresses to strains are needed, and these are provided by the material's constitutive relations. In this section, isotropic elastic materials are dealt with [2].

In the general case of a linear relation between components of the strain and stress tensors, we might propose a statement of the form:

$$\sigma_{ij} = L_{ijkl} (\varepsilon_{kl} - \varepsilon_{kl}^t) \quad (1.27)$$

where L_{ijkl} is a 4th order tensor and ε_{kl}^t is the initial (or eigen / stress-free) strain. Because indices kl do not appear in the equation after summation, they are called

“dummy indices”. Previous expression constitutes a sequence of nine equations, since each component of σ_{ij} is a linear combination of all the components of ε_{kl} . For instance

$$\sigma_{23} = L_{2311}\varepsilon_{11} + L_{2312}\varepsilon_{12} + \dots + L_{2333}\varepsilon_{33} \quad (1.28)$$

Based on each of the indices of L_{ijkl} taking on values from 1 to 3, we might expect 81 independent components in L . However, both the stress tensor and the strain tensor are symmetric ($\sigma_{ij} = \sigma_{ji}$ and $\varepsilon_{ij} = \varepsilon_{ji}$), we must also have $L_{ijkl} = L_{ijlk}$ and $L_{ijkl} = L_{jikl}$. These relations are called minor symmetries. The major symmetry of the stiffness tensor is expressed as $L_{ijkl} = L_{klij}$. This reduces the number of L components to 36, as can be seen from a linear relation between the pseudovector forms of the strain and stress [2]:

$$\begin{pmatrix} \sigma_x \\ \sigma_y \\ \sigma_z \\ \tau_{yz} \\ \tau_{xz} \\ \tau_{xy} \end{pmatrix} = \begin{bmatrix} L_{11} & L_{12} & \dots & L_{16} \\ L_{21} & L_{22} & \dots & L_{26} \\ \vdots & \vdots & \ddots & \vdots \\ L_{61} & L_{62} & \dots & L_{66} \end{bmatrix} \begin{pmatrix} \varepsilon_x \\ \varepsilon_y \\ \varepsilon_z \\ \gamma_{yz} \\ \gamma_{xz} \\ \gamma_{xy} \end{pmatrix} \quad (1.29)$$

or, using the Mandel notation:

$$\begin{pmatrix} \sigma_{11} \\ \sigma_{22} \\ \sigma_{33} \\ \sqrt{2}\sigma_{23} \\ \sqrt{2}\sigma_{13} \\ \sqrt{2}\sigma_{12} \end{pmatrix} = \begin{bmatrix} L_{1111} & L_{1122} & L_{1133} & \sqrt{2}L_{1112} & \sqrt{2}L_{1123} & \sqrt{2}L_{1113} \\ L_{2211} & L_{2222} & L_{2233} & \sqrt{2}L_{2212} & \sqrt{2}L_{2223} & \sqrt{2}L_{2213} \\ L_{3311} & L_{3322} & L_{3333} & \sqrt{2}L_{3312} & \sqrt{2}L_{3323} & \sqrt{2}L_{3313} \\ \sqrt{2}L_{1211} & \sqrt{2}L_{1222} & \sqrt{2}L_{1233} & 2L_{1212} & 2L_{1223} & 2L_{1213} \\ \sqrt{2}L_{2311} & \sqrt{2}L_{2322} & \sqrt{2}L_{2333} & 2L_{2312} & 2L_{2323} & 2L_{2313} \\ \sqrt{2}L_{1311} & \sqrt{2}L_{1322} & \sqrt{2}L_{1333} & 2L_{1312} & 2L_{1323} & 2L_{1313} \end{bmatrix} \begin{pmatrix} \varepsilon_{11} \\ \varepsilon_{22} \\ \varepsilon_{33} \\ \sqrt{2}\varepsilon_{23} \\ \sqrt{2}\varepsilon_{13} \\ \sqrt{2}\varepsilon_{12} \end{pmatrix} \quad (1.30)$$

It can be shown that the \mathbf{L} matrix in this form is also symmetric and therefore it contains only 21 independent elements.

If the material exhibits symmetry in its elastic response, the number of independent elements in the \mathbf{L} matrix can be further reduced. In the simplest case of an isotropic material, having the same stiffness in all directions, only two elements are independent – for example Young’s modulus (E) and Poisson’s ratio (ν). From these, so-called shear modulus can be calculated:

$$G = \frac{E}{2(1+\nu)} \quad (1.31)$$

If a body is loaded by the stress σ_x , the resulting deformation $\varepsilon_x = \sigma_x / E$ and the other normal components of strain are $\varepsilon_y = \varepsilon_z = -\nu\varepsilon_x = -\nu\sigma_x / E$. In the general stress-

state, the other normal strain components are derived analogically (however, the material must be isotropic):

$$\varepsilon_x = \frac{1}{E}(\sigma_x - \nu\sigma_y - \nu\sigma_z) \quad (1.32)$$

$$\varepsilon_y = \frac{1}{E}(-\nu\sigma_x + \sigma_y - \nu\sigma_z) \quad (1.33)$$

$$\varepsilon_z = \frac{1}{E}(-\nu\sigma_x - \nu\sigma_y + \sigma_z) \quad (1.34)$$

In case of isotropic material, each shear deformation is proportional to the corresponding shear stress with the constant of proportionality $1/G$:

$$\gamma_{xy} = \frac{\tau_{xy}}{G} = \frac{2(1+\nu)}{E}\tau_{xy} \quad (1.35)$$

$$\gamma_{xz} = \frac{\tau_{xz}}{G} = \frac{2(1+\nu)}{E}\tau_{xz} \quad (1.36)$$

$$\gamma_{yz} = \frac{\tau_{yz}}{G} = \frac{2(1+\nu)}{E}\tau_{yz} \quad (1.37)$$

The six above equations can be written in the matrix form (using the Mandel notation and therefore with the last 3 diagonal terms divided by 2) as

$$\begin{Bmatrix} \varepsilon_x \\ \varepsilon_y \\ \varepsilon_z \\ \gamma_{yz} \\ \gamma_{xz} \\ \gamma_{xy} \end{Bmatrix} = \frac{1}{E} \begin{bmatrix} 1 & -\nu & -\nu & 0 & 0 & 0 \\ -\nu & 1 & -\nu & 0 & 0 & 0 \\ -\nu & -\nu & 1 & 0 & 0 & 0 \\ 0 & 0 & 0 & 2(1+\nu) & 0 & 0 \\ 0 & 0 & 0 & 0 & 2(1+\nu) & 0 \\ 0 & 0 & 0 & 0 & 0 & 2(1+\nu) \end{bmatrix} \begin{Bmatrix} \sigma_x \\ \sigma_y \\ \sigma_z \\ \tau_{yz} \\ \tau_{xz} \\ \tau_{xy} \end{Bmatrix} \quad (1.38)$$

which can be written in compact form as

$$\boldsymbol{\varepsilon} = \mathbf{M}\boldsymbol{\sigma} \quad (1.39)$$

where \mathbf{M} is the elastic compliance matrix. By inversion, we get the generalized Hook's law:

$$\boldsymbol{\sigma} = (\mathbf{M})^{-1}\boldsymbol{\varepsilon} = \mathbf{L}\boldsymbol{\varepsilon} \quad (1.40)$$

where

$$\mathbf{L} = \frac{E}{(1+\nu)(1-2\nu)} \begin{bmatrix} 1-\nu & \nu & \nu & 0 & 0 & 0 \\ \nu & 1-\nu & \nu & 0 & 0 & 0 \\ \nu & \nu & 1-\nu & 0 & 0 & 0 \\ 0 & 0 & 0 & 2(0.5-\nu) & 0 & 0 \\ 0 & 0 & 0 & 0 & 2(0.5-\nu) & 0 \\ 0 & 0 & 0 & 0 & 0 & 2(0.5-\nu) \end{bmatrix} \quad (1.41)$$

is the elastic stiffness matrix of an isotropic material (using the Mandel notation and therefore with the last 3 diagonal terms multiplied by 2).

2 Hydrostatic and Deviatoric Components

2.1 Hydrostatic and Deviatoric Stresses

A state of hydrostatic compression is the one in which no shear stresses exist and where all the normal stresses are equal. For this stress state it is obviously true that

$$\sigma_m = \frac{\sigma_{11} + \sigma_{22} + \sigma_{33}}{3} = \frac{1}{3} \sigma_{kk} \quad (2.01)$$

This quantity (so called mean stress) is one third of invariant I_1 (so called hydrostatic or volumetric stress), which is a reflection of hydrostatic pressure being the same in all directions, not varying with axis rotations.

The stress tensor is then composed of the hydrostatic part and the deviatoric part:

$$\sigma_{ij} = \frac{1}{3} \sigma_{kk} \delta_{ij} + s_{ij} \quad (2.02)$$

where the symbol δ_{ij} is the Kronecker delta, which is defined as

$$\delta_{ij} = \begin{cases} 1 & \text{if } i = j \\ 0 & \text{if } i \neq j \end{cases} \quad (2.03)$$

The hydrostatic stress-state is defined as follows:

$$\boldsymbol{\sigma} = \begin{bmatrix} \sigma_m & 0 & 0 \\ 0 & \sigma_m & 0 \\ 0 & 0 & \sigma_m \end{bmatrix} \quad (2.04)$$

and the deviatoric stress state is then

$$\mathbf{s} = \begin{bmatrix} \sigma_{11} - \sigma_m & \sigma_{12} & \sigma_{13} \\ \sigma_{21} & \sigma_{22} - \sigma_m & \sigma_{23} \\ \sigma_{31} & \sigma_{32} & \sigma_{33} - \sigma_m \end{bmatrix} \quad (2.05)$$

The hydrostatic (volumetric) stress is related to the change of volume of a material during deformation, while the deviatoric part is responsible for the distortion. This concept is also convenient because the material responds to these stress components in very different ways. For instance, plastic and viscous behavior is caused dominantly by the distortional components, with the hydrostatic component causing only an elastic deformation [2].

The graphical representation of the stress tensor decomposition is shown in the following figure:

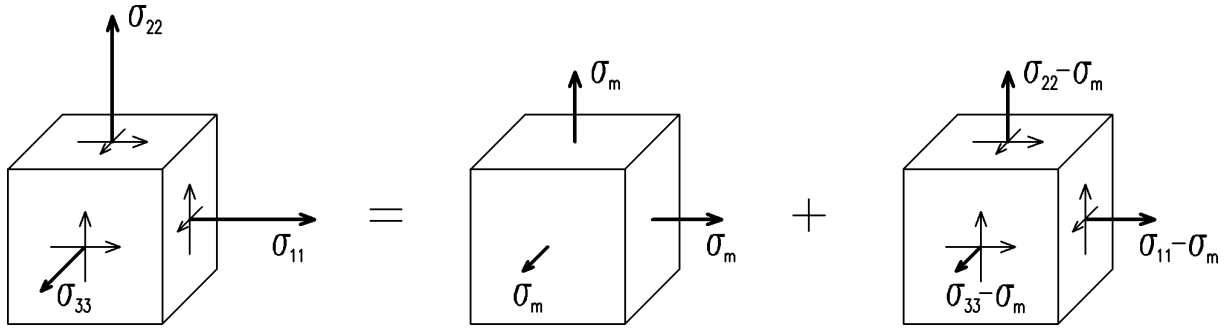


Fig. 2.1: Decomposition of stress in hydrostatic and deviatoric part

2.2 Hydrostatic and Deviatoric Strains

In cubical element, originally of volume abc , subjected to normal strains in all three directions, the change in the element's volume is

$$\begin{aligned} \frac{\Delta V}{V} &= \frac{a'b'c' - abc}{abc} = \frac{a(1 + \varepsilon_x)b(1 + \varepsilon_y)c(1 + \varepsilon_z) - abc}{abc} = \\ &= (1 + \varepsilon_x)(1 + \varepsilon_y)(1 + \varepsilon_z) - 1 \approx \varepsilon_x + \varepsilon_y + \varepsilon_z \end{aligned} \quad (2.06)$$

where products of strains are neglected. The volumetric strain is therefore the sum of the diagonal elements in the strain tensor (also called trace of the matrix, or $\text{Tr}(\boldsymbol{\varepsilon})$). In the index notation, this can be written simply as

$$\varepsilon_V = \frac{\Delta V}{V} = \varepsilon_{kk} \quad (2.07)$$

Similarly to mean stress σ_m , the mean strain is calculated as

$$\varepsilon_m = \frac{\varepsilon_{11} + \varepsilon_{22} + \varepsilon_{33}}{3} = \frac{1}{3} \varepsilon_{kk} \quad (2.08)$$

and the strain tensor is then composed of the hydrostatic and deviatoric part:

$$\varepsilon_{ij} = \frac{1}{3} \varepsilon_{kk} \delta_{ij} + e_{ij} \quad (2.09)$$

The hydrostatic strain is defined as follows:

$$\boldsymbol{\varepsilon} = \begin{bmatrix} \varepsilon_m & 0 & 0 \\ 0 & \varepsilon_m & 0 \\ 0 & 0 & \varepsilon_m \end{bmatrix} \quad (2.10)$$

and the deviatoric part is obtained by subtraction of ε_m from the diagonal terms from the strain tensor:

$$\mathbf{e} = \begin{bmatrix} \varepsilon_{11} - \varepsilon_m & \varepsilon_{12} & \varepsilon_{13} \\ \varepsilon_{21} & \varepsilon_{22} - \varepsilon_m & \varepsilon_{23} \\ \varepsilon_{31} & \varepsilon_{32} & \varepsilon_{33} - \varepsilon_m \end{bmatrix} \quad (2.11)$$

2.3 Constitutive Relations

Since ε_V is a relative change of volume, it must be independent of the coordinate system (therefore, it is so called invariant). The relation between volumetric strain and mean stress can be derived as follows:

$$\begin{aligned} \varepsilon_V &= \frac{1}{E}(\sigma_x - \nu\sigma_y - \nu\sigma_z) + \frac{1}{E}(-\nu\sigma_x + \sigma_y - \nu\sigma_z) + \frac{1}{E}(-\nu\sigma_x - \nu\sigma_y + \sigma_z) = \\ &= \frac{1-2\nu}{E}(\sigma_x + \sigma_y + \sigma_z) = \frac{3(1-2\nu)}{E} \frac{(\sigma_x + \sigma_y + \sigma_z)}{3} = \frac{\sigma_m}{K} \end{aligned} \quad (2.12)$$

where

$$K = \frac{E}{3(1-2\nu)} \quad (2.13)$$

is so called bulk modulus. The bulk modulus is the stiffness parameter that connects the mean hydrostatic stress σ_m with the volumetric strain ε_V . Note that as $\nu \rightarrow 0,5$, $K \rightarrow \infty$. That is, the material becomes infinitely stiff as Poisson's ratio approaches 0,5. Values of Poisson's ratio greater than 0,5 are not possible since such values imply that a tensile hydrostatic stress would cause a volumetric contraction. The volumetric change is proportional to the mean stress only in case of an isotropic material.

The normal component of the deviatoric deformation e_x can be expressed as

$$\begin{aligned} e_x &= \varepsilon_x - \varepsilon_m = \frac{1}{E}(\sigma_x - \nu\sigma_y - \nu\sigma_z) - \frac{1}{3K}\sigma_m = \\ &= \frac{1}{E} [s_x + \sigma_m - \nu(s_y + \sigma_m) - \nu(s_z + \sigma_m)] - \frac{1-2\nu}{E}\sigma_m \\ &= \frac{1}{E}(s_x - \nu s_y - \nu s_z) \end{aligned} \quad (2.14)$$

and since

$$\begin{aligned} s_x + s_y + s_z &= (\sigma_x - \sigma_m) + (\sigma_y - \sigma_m) + (\sigma_z - \sigma_m) = \sigma_x + \sigma_y + \sigma_z - 3\sigma_m = \\ &= 3\sigma_m - 3\sigma_m = 0 \end{aligned} \quad (2.15)$$

the sum of the deviatoric normal components is equal to zero. Therefore

$$\nu s_x = -\nu s_y - \nu s_z \quad (2.16)$$

and

$$e_x = \frac{1}{E}(s_x + \nu s_x) = \frac{1+\nu}{E}s_x = \frac{s_x}{2G} \quad (2.17)$$

The same relation holds for the other normal components of the deviatoric strain tensor as well. The shear strain components are (as mentioned before) related to the shear stress by the shear modulus G without factor 2. For instance the first shear component:

$$\gamma_{xy} = \frac{2(1+\nu)}{E}\tau_{xy} = \frac{\tau_{xy}}{G} \quad (2.18)$$

2.3.1 Index Notation, Lamé's Constants

For the diagonal terms in the strain tensor, for instance the strain ε_{11} , the strain-stress relationship can be expressed as

$$\varepsilon_{11} = \frac{1}{E}\sigma_{11} - \frac{1}{E}\nu(\sigma_{22} + \sigma_{33}) = \frac{(1+\nu)}{E}\sigma_{11} - \frac{1}{E}\nu(\sigma_{11} + \sigma_{22} + \sigma_{33}) \quad (2.19)$$

which can be, using the index notation, for all normal strains expressed as

$$\varepsilon_{ij} = \frac{(1+\nu)}{E}\sigma_{ij} - \frac{\nu}{E}\sigma_{kk} \quad \text{if } i = j \quad (2.20)$$

For the shear components of the stress tensor, for instance the strain ε_{12} , the strain-stress relationship can be expressed as

$$\varepsilon_{12} = \frac{(1+\nu)}{E}\sigma_{12} \quad (2.21)$$

which can be, using the index notation, for all shear strains expressed as

$$\varepsilon_{ij} = \frac{(1+\nu)}{E}\sigma_{ij} \quad \text{if } i \neq j \quad (2.22)$$

The previous equations (for normal and shear strains) can be written in a single expression by making use of the Kronecker delta:

$$\varepsilon_{ij} = \frac{(1+\nu)}{E} \sigma_{ij} - \frac{\nu}{E} \sigma_{kk} \delta_{ij} \quad (2.23)$$

The required form of the stress-strain relationship (dependence of stress on strains), using so-called Lamé's constants μ and λ has a form:

$$\sigma_{ij} = 2\mu\varepsilon_{ij} + \lambda\delta_{ij}\varepsilon_{kk} \quad (2.24)$$

In order to establish the relationship between Lamé's constants, Young's modulus and Poisson's ratio, it is necessary to compare the two forms of the constitutive equations for an isotropic elastic material with the previous equation. However, in order to make that comparison, the equations for strain-stress relationship must be inverted, because the previous equation expresses the stress components in terms of the strain components.

By simple arrangement, the following equation can be obtained:

$$\sigma_{kk} = \frac{E}{(1-2\nu)} \varepsilon_{kk} \quad (2.25)$$

and since we know that

$$\sigma_{ij} = \frac{E}{(1+\nu)} \left(\varepsilon_{ij} + \frac{\nu}{E} \sigma_{kk} \delta_{ij} \right) = \frac{E}{(1+\nu)} \varepsilon_{ij} + \frac{\nu}{(1+\nu)} \sigma_{kk} \delta_{ij} \quad (2.26)$$

where the σ_{kk} can be then substituted as follows:

$$\sigma_{ij} = \frac{E}{(1+\nu)} \varepsilon_{ij} + \frac{E\nu}{(1+\nu)(1-2\nu)} \varepsilon_{kk} \delta_{ij} \quad (2.27)$$

Therefore, the Lamé's constants can be expressed as

$$\mu = G = \frac{E}{2(1+\nu)} \quad (2.28)$$

and

$$\lambda = \frac{E\nu}{(1+\nu)(1-2\nu)} = K - \frac{2}{3} G \quad (2.29)$$

in terms of E , ν , K and G .

2.3.2 Tensorial Notation

In tensorial notation, there is needed the use of the unit fourth-order tensor, I_{ijkl} , with components:

$$I_{ijkl} = \delta_{ik} \delta_{jl} \quad (2.30)$$

with Kronecker delta being called the unit second-order tensor. This tensor exhibits major symmetry but not minor symmetry, and it has the important property that $\mathbf{I} : \boldsymbol{\varepsilon} = \boldsymbol{\varepsilon} : \mathbf{I} = \boldsymbol{\varepsilon}$ for any second-order tensor $\boldsymbol{\varepsilon}$ [3].

Sometimes it is useful to work with the symmetrized unit fourth-order tensor, \mathbf{I}_S , which has components:

$$I_{ijkl}^S = \frac{(\delta_{ik} \delta_{jl} + \delta_{il} \delta_{jk})}{2} \quad (2.31)$$

This tensor exhibits minor and major symmetry but the identity $\mathbf{I} : \boldsymbol{\varepsilon} = \boldsymbol{\varepsilon} : \mathbf{I} = \boldsymbol{\varepsilon}$ holds only if the second-order tensor $\boldsymbol{\varepsilon}$ is symmetric [3].

The stiffness tensor in linear isotropic elasticity is expressed as

$$\mathbf{L}_e = \lambda \boldsymbol{\delta} \otimes \boldsymbol{\delta} + 2\mu \mathbf{I}_S \quad (2.32)$$

or in index notation as

$$\mathbf{L}_{ijkl}^e = \lambda \delta_{ik} \delta_{jl} + \mu (\delta_{ik} \delta_{jl} + \delta_{il} \delta_{jk}) \quad (2.33)$$

Using the tensorial notation, the generalized Hooke's law can be presented as

$$\boldsymbol{\sigma} = \mathbf{L}_e : \boldsymbol{\varepsilon} = \lambda \boldsymbol{\delta} \otimes \boldsymbol{\delta} : \boldsymbol{\varepsilon} + 2\mu \mathbf{I}_S : \boldsymbol{\varepsilon} = 3\lambda \boldsymbol{\delta} \varepsilon_V + 2\mu \boldsymbol{\varepsilon} \quad (2.34)$$

where

$$\varepsilon_V = \frac{1}{3} \boldsymbol{\delta} : \boldsymbol{\varepsilon} \quad (2.35)$$

is one third of the trace of the strain tensor, representing the relative change of volume. The volumetric part of the strain tensor is $\varepsilon_V \boldsymbol{\delta}$, and when we subtract it from the strain tensor, we obtain the deviatoric strain [3]:

$$\mathbf{e} = \boldsymbol{\varepsilon} - \boldsymbol{\delta} \varepsilon_V = \boldsymbol{\varepsilon} - \frac{1}{3} \boldsymbol{\delta} \otimes \boldsymbol{\delta} : \boldsymbol{\varepsilon} = \left(\mathbf{I}_S - \frac{1}{3} \boldsymbol{\delta} \otimes \boldsymbol{\delta} \right) : \boldsymbol{\varepsilon} = \mathbf{I}_D : \boldsymbol{\varepsilon} \quad (2.36)$$

Therefore the deviatoric projection tensor is

$$\mathbf{I}_D = \mathbf{I}_S - \frac{1}{3} \boldsymbol{\delta} \otimes \boldsymbol{\delta} \quad (2.37)$$

and the volumetric projection tensor is

$$\mathbf{I}_V = \frac{1}{3} \boldsymbol{\delta} \otimes \boldsymbol{\delta} \quad (2.38)$$

Then the volumetric-deviatoric decomposition of the strain tensor can be done as follows [3]:

$$\boldsymbol{\varepsilon} = \mathbf{I}_S : \boldsymbol{\varepsilon} = (\mathbf{I}_V + \mathbf{I}_D) : \boldsymbol{\varepsilon} = \mathbf{I}_V : \boldsymbol{\varepsilon} + \mathbf{I}_D : \boldsymbol{\varepsilon} = \boldsymbol{\varepsilon}_{vol} + \boldsymbol{\varepsilon}_{dev} = \varepsilon_V \boldsymbol{\delta} + \mathbf{e} \quad (2.39)$$

And the stress tensor can be decomposed in the same way:

$$\boldsymbol{\sigma} = \mathbf{I}_S : \boldsymbol{\sigma} = (\mathbf{I}_V + \mathbf{I}_D) : \boldsymbol{\sigma} = \mathbf{I}_V : \boldsymbol{\sigma} + \mathbf{I}_D : \boldsymbol{\sigma} = \boldsymbol{\sigma}_{vol} + \boldsymbol{\sigma}_{dev} = \sigma_V \boldsymbol{\delta} + \mathbf{s} \quad (2.40)$$

where

$$\sigma_V = \mathbf{I}_V : \boldsymbol{\sigma} = \frac{1}{3} \boldsymbol{\delta} : \boldsymbol{\sigma} \quad (2.41)$$

is the mean stress and

$$\mathbf{s} = \mathbf{I}_D : \boldsymbol{\sigma} = \boldsymbol{\sigma} - \sigma_V \boldsymbol{\delta} \quad (2.42)$$

is the stress deviator.

The elastic stiffness tensor can also be decomposed into its volumetric and deviatoric part. Realizing that

$$\boldsymbol{\delta} \otimes \boldsymbol{\delta} = 3\mathbf{I}_V \quad (2.43)$$

we can rewrite the stiffness tensor in linear isotropic elasticity as

$$\begin{aligned} \mathbf{L}_e &= \lambda \boldsymbol{\delta} \otimes \boldsymbol{\delta} + 2\mu \mathbf{I}_S = 3\lambda \mathbf{I}_V + 2\mu (\mathbf{I}_V + \mathbf{I}_D) = \\ &= (3\lambda + 2\mu) \mathbf{I}_V + 2\mu \mathbf{I}_D = 3K \mathbf{I}_V + 2G \mathbf{I}_D \end{aligned} \quad (2.44)$$

because the coefficient $(3\lambda + 2\mu)$ is recognized as three times bulk modulus K and $\mu = G =$ shear modulus. The generalized Hooke's law [3]:

$$\boldsymbol{\sigma} = \mathbf{L}_e : \boldsymbol{\varepsilon} = (3K \mathbf{I}_V + 2G \mathbf{I}_D) : \boldsymbol{\varepsilon} = 3K \mathbf{I}_V : \boldsymbol{\varepsilon} + 2G \mathbf{I}_D : \boldsymbol{\varepsilon} = 3K \varepsilon_V \boldsymbol{\delta} + 2G \mathbf{e} \quad (2.45)$$

is split into the volumetric and deviatoric part:

$$\sigma_V = 3K \varepsilon_V \quad \text{and} \quad \mathbf{s} = 2G \mathbf{e} \quad (2.46)$$

2.3.3 Engineering Notation

While the tensorial notation is useful in theoretical derivations, for developing a numerical algorithm that should be implemented into a computer code, it is more convenient to store the stress and strain components in one-dimensional arrays (pseudovectors) and stiffness moduli in matrices [3].

The normal components are usually arranged in a natural order, i.e. σ_x followed by σ_y and σ_z . For the shear components, it is possible to use order, but the selected convention must be used throughout the entire project [3]. One possibility is to set

$$\boldsymbol{\sigma} = \begin{Bmatrix} \sigma_x \\ \sigma_y \\ \sigma_z \\ \sqrt{2} \tau_{yz} \\ \sqrt{2} \tau_{xz} \\ \sqrt{2} \tau_{xy} \end{Bmatrix} = \begin{Bmatrix} \sigma_{11} \\ \sigma_{22} \\ \sigma_{33} \\ \sqrt{2} \sigma_{23} \\ \sqrt{2} \sigma_{13} \\ \sqrt{2} \sigma_{12} \end{Bmatrix} \quad \text{and} \quad \boldsymbol{\varepsilon} = \begin{Bmatrix} \varepsilon_x \\ \varepsilon_y \\ \varepsilon_z \\ \sqrt{2} \gamma_{yz} \\ \sqrt{2} \gamma_{xz} \\ \sqrt{2} \gamma_{xy} \end{Bmatrix} = \begin{Bmatrix} \varepsilon_{11} \\ \varepsilon_{22} \\ \varepsilon_{33} \\ \sqrt{2} 2\varepsilon_{23} \\ \sqrt{2} 2\varepsilon_{13} \\ \sqrt{2} 2\varepsilon_{12} \end{Bmatrix} \quad (2.47)$$

The engineering shear component γ_{xy} is twice the tensorial shear strain because then the energy product

$$\boldsymbol{\sigma} : \boldsymbol{\varepsilon} = \sigma_{ij} \varepsilon_{ij} \quad (2.48)$$

can be simply replaced in the engineering notation by a simple scalar product of column vectors, $\boldsymbol{\sigma}^T \boldsymbol{\varepsilon}$.

However, the double contraction in evaluation of the tensorial norm defined as

$$\|\boldsymbol{\sigma}\|_{\sigma} = \sqrt{\boldsymbol{\sigma} : \boldsymbol{\sigma}} \quad (2.49)$$

resulting in

$$\begin{aligned} \boldsymbol{\sigma} : \boldsymbol{\sigma} &= \sigma_{ij} \sigma_{ij} = \sigma_{11}^2 + \sigma_{12}^2 + \sigma_{13}^2 + \dots + \sigma_{31}^2 + \sigma_{32}^2 + \sigma_{33}^2 = \\ &= \sigma_{11}^2 + \sigma_{22}^2 + \sigma_{33}^2 + 2(\sigma_{23}^2 + \sigma_{13}^2 + \sigma_{12}^2) \end{aligned} \quad (2.50)$$

is equal to the pseudovector multiplication

$$\boldsymbol{\sigma}^T \boldsymbol{\sigma} = \sigma_{11}^2 + \sigma_{22}^2 + \sigma_{33}^2 + 2\sigma_{23}^2 + 2\sigma_{13}^2 + 2\sigma_{12}^2 \quad (2.51)$$

only if we multiply the shear components in the pseudovector by the factor of $\sqrt{2}$ (Mandel notation). Otherwise (using the Voigt notation) the diagonal scaling matrix has to be inserted:

$$\|\boldsymbol{\sigma}\|_{\sigma} = \sqrt{\boldsymbol{\sigma}^T \mathbf{P} \boldsymbol{\sigma}} \quad (2.52)$$

where the scaling matrix \mathbf{P} has the following form:

$$\mathbf{P} = \text{diag}[1 \ 1 \ 1 \ 2 \ 2 \ 2] \quad (2.53)$$

Such scaling matrix leaves the normal components as they are and doubles the shear components.

When calculating the norm of the strain tensor, using the Voigt notation, it is also necessary to insert a scaling matrix, but not the same one as for two stress-like tensors. Since the shear components have already been doubled, the corresponding scaling factors are now 0.5 instead of 2. Therefore, it turns out that the appropriate scaling matrix is the inverse of \mathbf{P} and the tensorial norm of $\boldsymbol{\varepsilon}$ is in the engineering notation evaluated as

$$\|\boldsymbol{\varepsilon}\|_{\varepsilon} = \sqrt{\boldsymbol{\varepsilon}^T \mathbf{P}^{-1} \boldsymbol{\varepsilon}} \quad \text{where} \quad \mathbf{P}^{-1} = \text{diag}[1 \ 1 \ 1 \ 0.5 \ 0.5 \ 0.5] \quad (2.54)$$

However, if the Mandel notation is used, the scaling matrix equals to 1.

For the purpose of the volumetric-deviatoric decomposition, the engineering counterpart of the unit second-order tensor (Kronecker delta) is established as

$$\boldsymbol{\delta} = \{1 \ 1 \ 1 \ 0 \ 0 \ 0\}^T \quad (2.55)$$

The volumetric-deviatoric decomposition is in the engineering notation based on projection matrices

$$\mathbf{I}_V = \frac{1}{3} \boldsymbol{\delta} \boldsymbol{\delta}^T \quad (2.56)$$

and

$$\mathbf{I}_D = \mathbf{I} - \mathbf{I}_V = \mathbf{I} - \frac{1}{3} \boldsymbol{\delta} \boldsymbol{\delta}^T \quad (2.57)$$

with \mathbf{I} representing the identity matrix. Using the Mandel notation, the elastic stiffness matrix can be simply expressed by means of the volumetric and deviatoric projection matrices as follows:

$$\mathbf{L}_e = 3K\mathbf{I}_V + 2G\mathbf{I}_D \quad (2.58)$$

The generalized Hook's law

$$\boldsymbol{\sigma} = (3K\mathbf{I}_V + 2G\mathbf{I}_D) \boldsymbol{\varepsilon} \quad (2.59)$$

can be then split into the volumetric and deviatoric part:

$$\sigma_V = 3K\varepsilon_V \quad \text{and} \quad \mathbf{s} = 2G\mathbf{e} \quad (2.60)$$

3 Stiffness Homogenization

Many materials are inhomogeneous, i.e., they consist of dissimilar constituents (phases) that are distinguishable at some small length scale. The behavior of inhomogeneous materials is determined, on the one hand, by the relevant materials properties of the constituents and, on the other hand, by their geometry and topology (phase arrangement) [5].

Defects in an elastic material give rise to inhomogeneous stress and strain fields by which the defects can be characterized. Equivalence between an inhomogeneous material and some homogeneous material with a certain eigenstrain or eigenstress distribution can be established [5].

3.1 Eigenstrain

Since the eigenstrain is not caused by stress, eigenstrains are also referred to as stress-free transformation strains (superscript t). Formally, all kinds of strain, which may prevail in a material in the absence of stress, can be interpreted as eigenstrains; typical examples are thermal or plastic strains. In the framework of infinitesimal deformations the total strains ε_{ij} are the sum of elastic strains $\varepsilon^e_{ij} = M_{ijkl} \sigma_{kl}$ and the eigenstrains: $\varepsilon_{ij} = \varepsilon^e_{ij} + \varepsilon^t_{ij}$. The stress-strain relationship is then [4]

$$\sigma_{ij} = L_{ijkl} (\varepsilon_{kl} - \varepsilon^t_{kl}) \quad (3.01)$$

3.1.1 Inclusions

The phase transformation in solids, where atomic rearrangements change the geometry of the lattice, gives rise to spatial distribution of eigenstrain $\varepsilon^t_{ij}(\mathbf{x})$.

If nonvanishing eigenstrains prevail, only in some bounded subregion Ω of the homogeneous material, this region is called an inclusion and the surrounding material is called a matrix. It has to be emphasized that the elastic properties of an inclusion and the matrix are the same; otherwise the region Ω would be called an inhomogeneity [4].

3.1.2 Eshelby's Solution

Probably J.D. Eshelby (1916-1981) has found the most important analytical solution of micromechanics. It is valid for an unbounded domain which contains an ellipsoidal inclusion $\Omega^{(r)}$ with principal axes a_i .

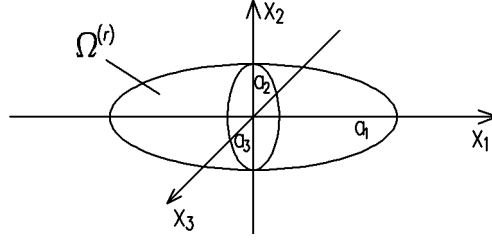


Fig. 3.1: Ellipsoidal inclusion in an unbounded domain

If the eigenstrains in the inclusion are constant ($\varepsilon_{ij}^t = \text{const.}$) then the remarkable result holds that the total strains ε_{ij} inside the inclusion are constant as well. Via fourth-order Eshelby's tensor S_{ijkl} they depend linearly on the eigenstrains [4]:

$$\varepsilon_{ij} = S_{ijkl} \varepsilon_{kl}^t = \text{const} \quad \text{in } \Omega^{(r)} \quad (3.02)$$

The Eshelby's tensor is symmetric in the first and second pair of indices, but in general it is not, symmetric with regard to an exchange of these pairs (exhibits the minor but not the major symmetry) [4]:

$$S_{ijkl} = S_{jilk} = S_{ijlk}, \quad S_{ijkl} \neq S_{klij} \quad (3.03)$$

In case of an isotropic material, its components depend only on Poisson's ratio ν , the ratios of the principal axes a_i , and their orientation with respect to some Cartesian coordinate system. The respective expressions are very long and can be found in literature (e.g., Mura, 1982; Kachanov et al., 2003).

The solution by Eshelby (1957) holds for an arbitrary anisotropic material. Yet, only in case of an isotropic material is a closed-form representation of the tensor S_{ijkl} , and the fields outside the inclusion, possible. The Eshelby solution for ellipsoidal inclusions is of fundamental importance for analytical homogenization techniques.

Starting from the general ellipsoid various special cases can be derived. For instance, the two-dimensional solution for an infinitely long cylinder of elliptic cross section in plane strain is obtained from the limit process $a_3 \rightarrow \infty$ [4].

For a spherical inclusion ($a_i = a$) in an isotropic material the dependence on the principal axes and their orientation vanishes (geometric isotropy) and the Eshelby tensor reduces to [4]

$$S_{ijkl} = \alpha^{(0)} \frac{1}{3} \delta_{ij} \delta_{kl} + \beta^{(0)} \left(I_{ijkl} - \frac{1}{3} \delta_{ij} \delta_{kl} \right) = \alpha^{(0)} \mathbf{I}_V + \beta^{(0)} \mathbf{I}_D \quad (3.04)$$

where

$$\alpha^{(0)} = \frac{1 + \nu^{(0)}}{3(1 - \nu^{(0)})} = \frac{3K^{(0)}}{3K^{(0)} + 4\mu^{(0)}} \quad \text{and} \quad \beta = \frac{2(4 - 5\nu^{(0)})}{15(1 - \nu^{(0)})} = \frac{6(K^{(0)} + 2\mu^{(0)})}{5(3K^{(0)} + 4\mu^{(0)})} \quad (3.05)$$

are scalar parameters. The superscript (0) stands for the matrix and (r) is later used for a representation of other components (inhomogeneities). The entire (i.e., elastic and geometric) isotropy of the problem then allows the decomposition into volumetric and deviatoric strain, which highlights the meaning of the parameters a and β [4]:

$$\varepsilon_{kk} = \alpha \varepsilon_{kk}^t \quad \text{and} \quad \varepsilon_{ij} = \beta \varepsilon_{ij}^t \quad \text{in } \Omega^{(r)} \quad (3.06)$$

Therefore the fourth rank Eshelby tensor turns out to be isotropic when the shape of the inclusion is spherical and can be characterized by a and β (representing the hydrostatic and the deviatoric parts of the constraint, respectively).

3.2 Inhomogeneities

The second class of defects, which instead of eigenstrains in a homogeneous material are characterized by inhomogeneous, i.e., spatially varying, material properties are called inhomogeneities. We first describe these defects by an equivalent eigenstrain in some homogeneous comparison material in order to then apply again Eshelby's result [4].

This strategy involves replacing an actual perfectly bounded inhomogeneity (superscript (i)), subjected to the eigenstrain ε^t , with an equivalent (fictitious) homogeneous inclusion (superscript (m)) with the equivalent eigenstrain ε^τ . This equivalent eigenstrain must be chosen in such a way, that the inhomogeneity and the equivalent homogeneous inclusion attain the same stress state $\sigma^{(i)}$ and the same constrained strain ε^c (Eshelby, 1957).

When $\sigma^{(i)}$ is expressed in terms of the elastic strain in the inhomogeneity, the following equality holds:

$$\sigma^{(i)} = \mathbf{L}^{(i)} : (\varepsilon^c - \varepsilon^t) = \mathbf{L}^{(m)} : (\varepsilon^c - \varepsilon^\tau) \quad (3.07)$$

Here, the differences $\varepsilon^c - \varepsilon^t$ and $\varepsilon^c - \varepsilon^\tau$ are the elastic strains in the inhomogeneity and the equivalent homogeneous inclusion, respectively. We can express the constrained strain using the Eshelby tensor as $\varepsilon^c = \mathbf{S} \varepsilon^\tau$. Hence, the equation for the stress $\sigma^{(i)}$ can be also written as [5]

$$\sigma^{(i)} = \mathbf{L}^{(i)} : (\mathbf{S} : \varepsilon^\tau - \varepsilon^t) = \mathbf{L}^{(m)} : (\mathbf{S} - \mathbf{I}) : \varepsilon^\tau \quad (3.08)$$

where \mathbf{I} is the symmetric fourth-order unit tensor, which turns out to be the identity matrix in the Mandel notation.

By simple manipulation with the equation for $\sigma^{(i)}$, we can express the equivalent eigenstrain as a function of the stress-free eigenstrain ε^t in the real inclusion as

$$\varepsilon^\tau = [(\mathbf{L}^{(i)} - \mathbf{L}^{(m)}) : \mathbf{S} + \mathbf{L}^{(m)}]^{-1} : \mathbf{L}^{(i)} : \varepsilon^t \quad (3.09)$$

This, in turn, allows the stress in the inhomogeneity, $\boldsymbol{\sigma}^{(i)}$, to be expressed as

$$\boldsymbol{\sigma}^{(i)} = \mathbf{L}^{(m)} : (\mathbf{S} - \mathbf{I}) : \left[(\mathbf{L}^{(i)} - \mathbf{L}^{(m)}) : \mathbf{S} + \mathbf{L}^{(m)} \right]^{-1} : \mathbf{L}^{(i)} : \boldsymbol{\varepsilon}^t \quad (3.10)$$

If a perfectly bonded inhomogeneity in an infinite matrix is subjected to a uniform mechanical strain $\boldsymbol{\varepsilon}^a$ or external stress $\boldsymbol{\sigma}^a$, the strain in the inclusion is a superposition of the applied strain and of the term $\boldsymbol{\varepsilon}^c$ that accounts for the constraint effects of the surrounding matrix. The stress in the inhomogeneity is after such loading [5]:

$$\boldsymbol{\sigma}^{(i)} = \mathbf{L}^{(i)} : (\boldsymbol{\varepsilon}^a + \boldsymbol{\varepsilon}^c) = \mathbf{L}^{(m)} : (\boldsymbol{\varepsilon}^a + \boldsymbol{\varepsilon}^c - \boldsymbol{\varepsilon}^\tau) \quad (3.11)$$

corresponding to the strain

$$\boldsymbol{\varepsilon}^{(i)} = \boldsymbol{\varepsilon}^a + \boldsymbol{\varepsilon}^c = \boldsymbol{\varepsilon}^a + \mathbf{S} : \boldsymbol{\varepsilon}^\tau \quad (3.12)$$

On the basis of these relationships the strain in the inhomogeneity can be expressed as

$$\boldsymbol{\varepsilon}^{(i)} = \left[\mathbf{I} + \mathbf{S} : \mathbf{M}^{(m)} : (\mathbf{L}^{(i)} - \mathbf{L}^{(m)}) \right]^{-1} : \boldsymbol{\varepsilon}^a \quad (3.13)$$

And since the strain in the inhomogeneity is homogeneous (piecewise constant), $\boldsymbol{\varepsilon}^{(i)} = \langle \boldsymbol{\varepsilon}^{(i)} \rangle = \mathbf{E}^{(i)}$, the strain concentration factor according to Hill (1965), describing the relation between the strain inside the inhomogeneity and the external load, for dilute inhomogeneities is

$$\mathbf{A}_{dil}^{(i)} = \left[\mathbf{I} + \mathbf{S} : \mathbf{M}^{(m)} : (\mathbf{L}^{(i)} - \mathbf{L}^{(m)}) \right]^{-1} \quad (3.14)$$

By setting $\langle \boldsymbol{\varepsilon}^{(i)} \rangle = \mathbf{L}^{(i)} \langle \boldsymbol{\sigma}^{(i)} \rangle$ and using $\boldsymbol{\varepsilon}^a = \mathbf{M}^{(m)} \boldsymbol{\sigma}^a$, the dilute stress concentration factor can be found from the previous equation as [5]

$$\begin{aligned} \mathbf{B}_{dil}^{(i)} &= \mathbf{L}^{(i)} : \left[\mathbf{I} + \mathbf{S} : \mathbf{M}^{(m)} : (\mathbf{L}^{(i)} - \mathbf{L}^{(m)}) \right]^{-1} : \mathbf{L}^{(m)} = \\ &= \left[\mathbf{I} + \mathbf{L}^{(m)} : (\mathbf{I} - \mathbf{S}) : (\mathbf{M}^{(i)} - \mathbf{M}^{(m)}) \right]^{-1} \end{aligned} \quad (3.15)$$

It is convenient to change the superscripts m and i , used for the derivation of the dilute concentration factors, to 0 representing the matrix and r representing the inhomogeneities. Such notation allows for the homogenization of more than one inhomogeneity embedded in the matrix.

The total strain inside the inhomogeneity $\boldsymbol{\Omega}^{(r)}$ as a function of the external load $\boldsymbol{\varepsilon}^0$ (or equal macroscopic strain \mathbf{E}) is then

$$\mathbf{E}^{(r)} = \left[\mathbf{I} + \mathbf{S} : \mathbf{M}^{(0)} : (\mathbf{L}^{(r)} - \mathbf{L}^{(0)}) \right]^{-1} : \mathbf{E} = \mathbf{A}^{(r)} : \mathbf{E} \quad (3.16)$$

where $\mathbf{E}^{(r)}$ is the strain in the r^{th} phase, and if r attains the value 0, we get the strain in the matrix. The previous equation can be written using the index notation as

$$\mathbf{E}_{ij}^{(r)} = A_{ijkl}^{(r)} \mathbf{E}_{kl} \quad (3.17)$$

The total stress inside the inhomogeneity $\Omega^{(r)}$ as a function of the external load $\boldsymbol{\sigma}^0$ (or equal macroscopic stress $\boldsymbol{\Sigma}$) is

$$\boldsymbol{\Sigma}^{(r)} = [\mathbf{I} + \mathbf{S} : \mathbf{M}^{(0)} : (\mathbf{L}^{(r)} - \mathbf{L}^{(0)})] : \boldsymbol{\Sigma} = \mathbf{B}^{(r)} : \boldsymbol{\Sigma} \quad (3.18)$$

which can be written in the index notation as

$$\Sigma_{ij}^{(r)} = B_{ijkl}^{(r)} \Sigma_{kl} \quad (3.19)$$

where the fourth-order tensor \mathbf{B} is the stress concentration factor (also called a stress influence tensor).

3.3 Effective Elastic Properties

A macroscopically homogeneous material may have a heterogeneous microstructure at the microscopic level. Under certain conditions, the material can be described at the macroscopic level as homogeneous with spatially constant effective properties. This means that the microstructure is averaged; this micro-to-macro transition is called homogenization [5].

The suitable volume for homogenization is called “representative volume element” (RVE). The representative volume element must be big enough to include enough non-homogeneities of materials (statistically homogeneous distribution of the defects or heterogeneities), but small enough to have the stresses and strains within RVE uniform (size with respect to the analyzed detail of a structure).

3.3.1 Averaging

The macro-stresses and macro-strains, which characterize the mechanical state of the macroscopic material point, are defined as the volumetric averages of the microscopic fields:

$$\langle \sigma_{ij} \rangle = \Sigma_{ij} = \frac{1}{|\Omega|} \int_{\Omega} \sigma_{ij}(\mathbf{x}) d\mathbf{x} \quad (3.20)$$

for effective (average) stress in the volume Ω . Employing the divergence theorem (also known as the Gauss theorem, the Green theorem or per-partes integration in more dimensions) the macroscopic stress can also be expressed using integrals over the boundary $\partial\Omega$ (curve integrals) of the averaging domain Ω [4]:

$$\Sigma_{ij} = \frac{1}{|\Omega|} \int_{\partial\Omega} t_i x_j dA \quad (3.21)$$

The macro-strains are calculated as

$$\langle \varepsilon_{ij} \rangle = E_{ij} = \frac{1}{|\Omega|} \int_{\Omega} \varepsilon_{ij}(\mathbf{x}) d\mathbf{x} \quad (3.22)$$

which can be also expressed as [4]

$$E_{ij} = \frac{1}{2|\Omega|} \int_{\Omega} (u_{i,j} + u_{j,i}) dV = \frac{1}{2\Omega} \int_{\partial\Omega} (u_i n_j + u_j n_i) dA \quad (3.23)$$

Often a volume Ω of a heterogeneous material consists of n subdomains and a matrix with volume fractions

$$c^{(r)} = \frac{|\Omega^{(r)}|}{|\Omega|} \quad (r = 0, \dots, n) \quad (3.24)$$

where $r = 0$ is used for the matrix itself. Obviously then

$$\sum_{r=0}^n c^{(r)} = 1 \quad (3.25)$$

where the elastic properties $\mathbf{L}^{(r)}$ are piecewise constant. In case of such microstructure, consisting of discrete phases, we have

$$\Sigma_{ij} = \sum_{r=0}^n c^{(r)} \Sigma_{ij}^{(r)} \quad (3.26)$$

since

$$\begin{aligned} \Sigma_{ij} &= \frac{1}{|\Omega|} \int_{\Omega} \sigma_{ij}(\mathbf{x}) d\mathbf{x} = \frac{1}{|\Omega|} \left(\sum_{r=0}^n \int_{\Omega^{(r)}} \sigma_{ij}(\mathbf{x}) d\mathbf{x} \right) = \frac{1}{|\Omega|} \left(\frac{|\Omega^{(r)}|}{|\Omega^{(r)}|} \sum_{r=0}^n \int_{\Omega^{(r)}} \sigma_{ij}(\mathbf{x}) d\mathbf{x} \right) = \\ &= \sum_{r=0}^n c^{(r)} \Sigma_{ij}^{(r)} \end{aligned} \quad (3.27)$$

and analogously for the strains, it holds that

$$E_{ij} = \sum_{r=0}^n c^{(r)} E_{ij}^{(r)} \quad (3.28)$$

which means that the total stress (or strain) is the sum of phase stress (or strain) with the weight $c^{(r)}$.

3.3.2 Effective Elastic Constants

Analogous to the elasticity law on the microscopic level, the effective stiffness tensor is defined by the linear relation between the macro-stresses and macro-strains:

$$\Sigma_{ij} = L_{ijkl}^{eff} E_{kl} \quad (3.29)$$

The interpretation of the effective stiffness tensor as a material property is subjected to several conditions. It is, for instance, the equality of the average strain energy density $\langle U \rangle$ in the volume Ω when expressed by means of the microscopic and macroscopic quantities [4]:

$$\langle U \rangle = \left\langle \frac{1}{2} E_{ij}^{(r)} L_{ijkl} E_{kl}^{(r)} \right\rangle = \frac{1}{2} \langle E_{ij}^{(r)} \rangle L_{ijkl}^{eff} \langle E_{kl}^{(r)} \rangle = \frac{1}{2} E_{ij} L_{ijkl}^{eff} E_{kl} \quad (3.30)$$

This requirement, known as the Hill condition (Hill, 1963), can also be written in the form

$$\langle \sigma_{ij} \varepsilon_{ij} \rangle = \langle \sigma_{ij} \rangle \langle \varepsilon_{ij} \rangle \quad (3.31)$$

The relation between the applied (macroscopic) strains and stresses can be expressed as

$$\Sigma_{ij} = \sum_{r=0}^n c^{(r)} \Sigma_{ij}^{(r)} = \sum_{r=0}^n c^{(r)} L_{ijkl}^{(r)} E_{kl}^{(r)} = \sum_{r=0}^n c^{(r)} L_{ijkl}^{(r)} A_{klmn}^{(r)} E_{mn} = L_{ijmn}^{(eff)} E_{mn} \quad (3.32)$$

Therefore, the effective stiffness matrix (in the matrix notation) is calculated as follows:

$$\mathbf{L}^{eff} = \sum_{r=0}^n c^{(r)} \mathbf{L}^{(r)} \mathbf{A}^{(r)} \quad (3.33)$$

Analogously, the compliance matrix can be calculated as

$$\mathbf{M}^{eff} = \sum_{r=0}^n c^{(r)} \mathbf{M}^{(r)} \mathbf{B}^{(r)} \quad (3.34)$$

It can be proved that

$$\sum_{r=0}^n c^{(r)} \mathbf{A}^{(r)} = \mathbf{I} \quad \text{and} \quad \sum_{r=0}^n c^{(r)} \mathbf{B}^{(r)} = \mathbf{I} \quad (3.35)$$

where \mathbf{I} is the identity matrix, \mathbf{A} and \mathbf{B} are strain and stress concentration tensors, respectively. For a matrix with only one type of inhomogeneity, the combination of the previous equations results in the following expression:

$$\begin{aligned}\mathbf{L}^{eff} &= c^{(0)} \mathbf{L}^{(0)} \mathbf{A}^{(0)} + c^{(1)} \mathbf{L}^{(1)} \mathbf{A}^{(1)} = c^{(0)} \mathbf{L}^{(0)} \mathbf{A}^{(0)} + c^{(1)} \mathbf{L}^{(1)} (\mathbf{I} - \mathbf{A}^{(1)}) = \\ &= c^{(0)} \mathbf{L}^{(0)} \mathbf{A}^{(0)} + \mathbf{L}^{(1)} (\mathbf{I} - c^{(0)} \mathbf{A}^{(0)}) = \mathbf{L}^{(1)} + c^{(0)} (\mathbf{L}^{(0)} - \mathbf{L}^{(1)}) \mathbf{A}^{(0)}\end{aligned}\quad (3.36)$$

where the quantities with the superscript (0) represent a matrix and the quantities with the superscript (1) represent an inhomogeneity (also called reinforcement or defect). Using the same reasoning for the different boundary conditions (loading by the external load $\boldsymbol{\sigma}^0$) and for one type of inhomogeneity, the stiffness tensor can be derived as

$$\mathbf{L}^{eff} = [\mathbf{M}^{(1)} + c^{(0)} (\mathbf{M}^{(0)} - \mathbf{M}^{(1)}) : \mathbf{B}^{(0)}]^{-1} \quad (3.37)$$

3.3.3 Voigt and Reuss Approximation

In a homogeneous material, the boundary conditions lead to homogeneous (spatially constant) stress and strain fields. The first possibility are prescribed linear displacements $u_i = \varepsilon_{ij}^0 x_j$ and therefore $\boldsymbol{\varepsilon}^0 = \text{const} = \mathbf{E}$. The second possibility is loading by uniform tractions $t_i = \sigma_{ij}^0 n_j$ where $\boldsymbol{\sigma}^0 = \text{const} = \boldsymbol{\Sigma}$.

In case of a heterogeneous material, the simplest approximation is to assume the micro-fields to be constant, in accordance with the boundary conditions [4].

These approximations are exact only in one-dimensional special cases of different materials arranged "in parallel" (Voigt) or "in series" (Reuss). Despite obvious deficiencies, the simple approximations by Voigt and Reuss bear the advantage that they yield exact bounds for the true effective elastic constants of a heterogeneous material. It can be shown that [4]

$$K_{\text{Reuss}}^{eff} \leq K^{eff} \leq K_{\text{Voigt}}^{eff} \quad (3.38)$$

and

$$G_{\text{Reuss}}^{eff} \leq G^{eff} \leq G_{\text{Voigt}}^{eff} \quad (3.39)$$

3.3.3.1 Voigt Approximation

If according to Voigt (1889) the strains inside a volume Ω of a heterogeneous body are taken to be constant ($\boldsymbol{\varepsilon}^{(r)} = \mathbf{E} = \text{const}$), it is obvious that the influence tensor for Voigt approximation is $\mathbf{A} = \mathbf{1}$. The effective stiffness matrix (or tensor) is then approximated as follows:

$$\mathbf{L}_{\text{Voigt}}^{eff} = \langle \mathbf{L} \rangle = \sum_{r=0}^n c^{(r)} \mathbf{L}^{(r)} \quad (3.40)$$

In the special case of discrete phases of an isotropic material the above approximation leads to the effective bulk modulus

$$K_{\text{Voigt}}^{\text{eff}} = \sum_{r=0}^n c^{(r)} K^{(r)} \quad (3.41)$$

and shear modulus

$$G_{\text{Voigt}}^{\text{eff}} = \sum_{r=0}^n c^{(r)} G^{(r)} \quad (3.42)$$

However, if one of the phases is rigid (e.g., $L^{(1)} \rightarrow \infty$) one obtains $L^{\text{eff}} \rightarrow \infty$ from the Voigt approximation.

3.3.3.2 Reuss Approximation

Analogously, a constant stress field is assumed in the approximation according to Reuss (1929) ($\sigma^{(r)} = \Sigma = \text{const}$), which corresponds to $\mathbf{B} = 1$. The effective compliance matrix (or tensor) is then approximated as follows [4]:

$$\mathbf{M}_{\text{Reuss}}^{\text{eff}} = \langle \mathbf{M} \rangle = \sum_{r=0}^n c^{(r)} \mathbf{M}^{(r)} \quad (3.43)$$

In the special case of discrete phases of an isotropic material the above approximation leads to the effective bulk modulus

$$\frac{1}{K_{\text{Reuss}}^{\text{eff}}} = \sum_{r=0}^n \frac{c^{(r)}}{K^{(r)}} \quad (3.44)$$

and shear modulus

$$\frac{1}{G_{\text{Voigt}}^{\text{eff}}} = \sum_{r=0}^n \frac{c^{(r)}}{G^{(r)}} \quad (3.45)$$

However, in case of a matrix containing cavities or cracks the vanishing stiffness (e.g., $L^{(1)} \rightarrow 0$), leads to $L^{\text{eff}} \rightarrow 0$.

3.3.4 Dilute (Non-Interacting) Defect Distribution

The simplest situation for modeling is when the inhomogeneities or defects are so dilutely distributed in the homogeneous matrix that their interaction among each other and with the boundary of the RVE can be neglected (“dilute distribution”) [4].

As illustrated in Fig. 3.3, each inhomogeneity can be considered in an unbounded domain, subjected to a uniform far-field loading $\varepsilon^0 = \langle \varepsilon \rangle = \mathbf{E}$ or $\sigma^0 = \langle \sigma \rangle = \Sigma$. The

characteristic dimension of the inhomogeneities therefore has to be small, compared to their distance or to the distance from the boundary of the RVE. Although the solutions obtained under these idealizations are valid only for very small volume fractions ($c^{(r)} \ll 1$) they form the basis for important generalization [4].

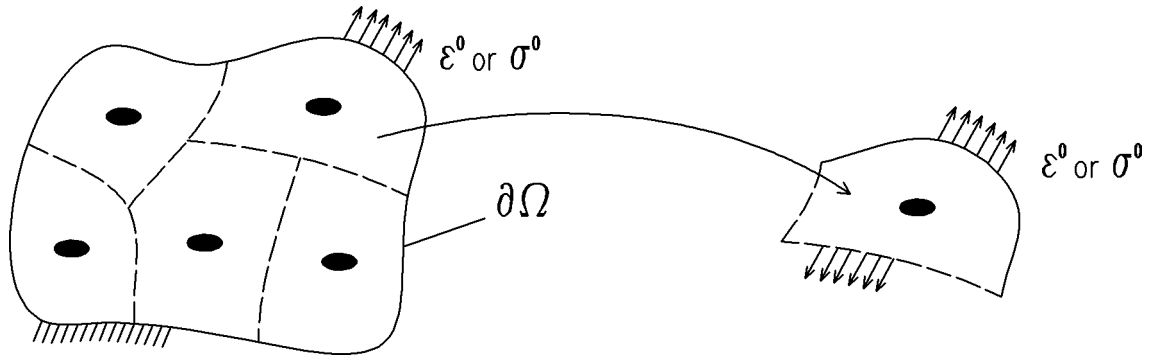


Fig. 3.3: Model of dilute phase distribution [4]

In case of an ellipsoidal inhomogeneity the strain inside the inhomogeneity $\Omega^{(r)}$ is constant and given by the influence tensor $\mathbf{A}^{(r)}$, which is calculated for each phase separately as

$$\mathbf{A}_{\text{dil}}^{(r)} = [\mathbf{I} + \mathbf{S}^{(0)} : \mathbf{M}^{(0)} : (\mathbf{L}^{(r)} - \mathbf{L}^{(0)})]^{-1} \quad (3.46)$$

where the Eshelby tensor (or matrix in engineering notation) depends on the matrix material.

3.3.5 Mori-Tanaka Model

The approximation of a dilute distribution of non-interacting defects is equivalent to the assumption that in a sufficient distance from each defect the constant strain field ϵ^0 or stress field σ^0 of the external loading prevails. This assumption is the starting point for a refinement of the model to account for an interaction of inhomogeneities (defects) [4].

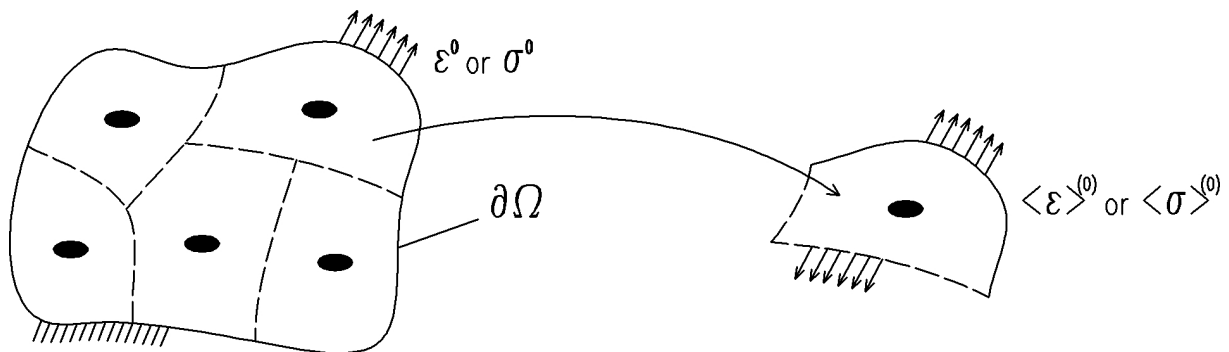


Fig. 3.4: Interaction of inhomogeneities in the Mori-Tanaka model [4]

In the Mori-Tanaka model (1973) the strain or stress field in the matrix is, in a sufficient distance from an inhomogeneity, approximated by the constant field $\langle \boldsymbol{\varepsilon} \rangle^M$ or the average stress $\langle \boldsymbol{\sigma} \rangle^M$ as illustrated in Fig. 3.4.

The loading of each phase then depends on the existence of other defects via the average matrix strain $\langle \boldsymbol{\varepsilon} \rangle^M = \mathbf{E}^{(0)}$ or the average matrix stress $\langle \boldsymbol{\sigma} \rangle^M = \boldsymbol{\Sigma}^{(0)}$. Fluctuations of the local fields are neglected in this approximation.

In the view of the idealized consideration of a single inhomogeneity in an unbounded matrix, subjected to effective loading $\langle \boldsymbol{\varepsilon} \rangle^M$ or $\langle \boldsymbol{\sigma} \rangle^M$, the Mori-Tanaka model formally equals that of a dilute distribution and allows the application of the already known concentration tensors from the dilute distribution model, $\mathbf{A}_{\text{dil}}^{(r)}$, to represent the average strain in inhomogeneity [4]:

$$\mathbf{E}^{(r)} = \mathbf{A}_{\text{dil}}^{(r)} \mathbf{E}^{(0)} \quad (3.47)$$

In order to determine the effective material properties the average defect strain needs to be represented as a function of the macroscopic quantities $\boldsymbol{\varepsilon}^0 = \langle \boldsymbol{\varepsilon} \rangle = \mathbf{E}$ or $\boldsymbol{\sigma}^0 = \langle \boldsymbol{\sigma} \rangle = \boldsymbol{\Sigma}$.

The total macroscopic strain is then

$$\begin{aligned} \mathbf{E} &= c^{(0)} \mathbf{E}^{(0)} + \sum_{r=1}^n c^{(r)} \mathbf{E}^{(r)} = c^{(0)} \mathbf{E}^{(0)} + \sum_{r=1}^n c^{(r)} \mathbf{A}_{\text{dil}}^{(r)} \mathbf{E}^{(0)} = \\ &= \left(c^{(0)} \mathbf{I} + \sum_{r=1}^n c^{(r)} \mathbf{A}_{\text{dil}}^{(r)} \right) \mathbf{E}^{(0)} \end{aligned} \quad (3.48)$$

For multi-phase materials consisting of a matrix (superscript 0) into which n inhomogeneity phases are embedded, the Mori-Tanaka models are based on the following relations:

$$\mathbf{E}^{(0)} = \mathbf{A}_{\text{MT}}^{(0)} \mathbf{E} \quad (3.49)$$

where

$$\mathbf{A}_{\text{MT}}^{(0)} = \left(c^{(0)} \mathbf{I} + \sum_{r=1}^n c^{(r)} \mathbf{A}_{\text{dil}}^{(r)} \right)^{-1} \quad (3.50)$$

is the Mori-Tanaka strain concentration factor. The strain in the individual inhomogeneities is then

$$\mathbf{E}^{(r)} = \mathbf{A}_{\text{dil}}^{(r)} : \mathbf{E}^{(0)} = \mathbf{A}_{\text{dil}}^{(r)} : \mathbf{A}_{\text{MT}}^{(0)} : \mathbf{E} \quad (3.51)$$

Analogously the stress concentration factor for Mori-Tanaka method takes the form

$$\mathbf{B}_{\text{MT}}^{(0)} = \left(c^{(0)} \mathbf{I} + \sum_{r=1}^n c^{(r)} \mathbf{B}_{\text{dil}}^{(r)} \right)^{-1} \quad (3.52)$$

and the stress in the individual inhomogeneities is

$$\boldsymbol{\Sigma}^{(r)} = \mathbf{B}_{\text{dil}}^{(r)} : \boldsymbol{\Sigma}^{(0)} = \mathbf{B}_{\text{dil}}^{(r)} : \mathbf{B}_{\text{MT}}^{(0)} : \boldsymbol{\Sigma} \quad (3.53)$$

The effective macroscopic elastic tensor is obtained as

$$\begin{aligned} \mathbf{L}^{\text{eff}} &= \sum_{r=0}^n c^{(r)} \mathbf{L}^{(r)} : \mathbf{A}^{(r)} = c^{(0)} \mathbf{L}^{(0)} : \mathbf{A}_{\text{MT}}^{(0)} + \sum_{r=1}^n c^{(r)} \mathbf{L}^{(r)} : \mathbf{A}_{\text{dil}}^{(r)} : \mathbf{A}_{\text{MT}}^{(0)} = \\ &= \left(c^{(0)} \mathbf{L}^{(0)} + \sum_{r=1}^n c^{(r)} \mathbf{L}^{(r)} : \mathbf{A}_{\text{dil}}^{(r)} \right) : \mathbf{A}_{\text{MT}}^{(0)} \end{aligned} \quad (3.54)$$

and the compliance elastic tensor as

$$\begin{aligned} \mathbf{M}^{\text{eff}} &= \sum_{r=0}^n c^{(r)} \mathbf{M}^{(r)} : \mathbf{B}^{(r)} = c^{(0)} \mathbf{M}^{(0)} : \mathbf{B}_{\text{MT}}^{(0)} + \sum_{r=1}^n c^{(r)} \mathbf{M}^{(r)} : \mathbf{B}_{\text{dil}}^{(r)} : \mathbf{B}_{\text{MT}}^{(0)} = \\ &= \left(c^{(0)} \mathbf{M}^{(0)} + \sum_{r=1}^n c^{(r)} \mathbf{M}^{(r)} : \mathbf{B}_{\text{dil}}^{(r)} \right) : \mathbf{B}_{\text{MT}}^{(0)} \end{aligned} \quad (3.55)$$

The Mori-Tanaka model, in contrast to the model of a dilute distribution, correctly covers the extreme cases of $c^{(r)} = 0$ and $c^{(r)} = 1$ (corresponding to homogeneous material) and therefore can formally be applied for arbitrary volume fractions $c^{(r)}$ [4].

In the special case of an isotropic matrix which contains isotropic spherical inhomogeneities the Mori-Tanaka model yields, irrespective of the spatial arrangement of the phases, an isotropic overall behavior with effective elastic constants. It is because the Eshelby tensor can be decomposed to its volumetric and deviatoric part. Using the equations (3.04), (3.51) and (3.55), which can be written in slightly different way, we get

$$\mathbf{L}^{\text{eff}} = \frac{c^{(0)} \mathbf{L}^{(0)} + \sum_{r=1}^n c^{(r)} \mathbf{L}^{(r)} : \mathbf{A}_{\text{dil}}^{(r)}}{c^{(0)} \mathbf{I} + \sum_{r=1}^n c^{(r)} \mathbf{A}_{\text{dil}}^{(r)}} \quad (3.56)$$

which can be decomposed to volumetric and deviatoric components as follows:

$$3K^{\text{eff}} \mathbf{I}_V + 2G^{\text{eff}} \mathbf{I}_D = \frac{c^{(0)} (3K^{(0)} \mathbf{I}_V + 2G^{(0)} \mathbf{I}_D) + \sum_{r=1}^n c^{(r)} (3K^{(r)} \mathbf{I}_V + 2G^{(r)} \mathbf{I}_D) : \mathbf{A}_{\text{dil}}^{(r)}}{c^{(0)} (\mathbf{I}_V + \mathbf{I}_D) + \sum_{r=1}^n c^{(r)} \mathbf{A}_{\text{dil}}^{(r)}} \quad (3.57)$$

where also the dilute strain concentration factor can be further decomposed as follows:

$$\begin{aligned}
\mathbf{A}_{\text{dil}}^{(r)} &= \left[\mathbf{I} + \mathbf{S}^{(0)} : \mathbf{M}^{(0)} : (\mathbf{L}^{(r)} - \mathbf{L}^{(0)}) \right]^{-1} = \\
&= \frac{1}{\mathbf{I}_V + \mathbf{I}_D + \frac{(\alpha \mathbf{I}_V + \beta \mathbf{I}_D) [3(K^{(r)} - K^{(0)}) \mathbf{I}_V + 2(G^{(r)} - G^{(0)}) \mathbf{I}_D]}{3K^{(0)} \mathbf{I}_V + 2G^{(0)} \mathbf{I}_D}} \quad (3.58)
\end{aligned}$$

and since the volumetric and deviatoric components are independent of each other, the effective bulk modulus can be, after a simple manipulation with the previous two equations, expressed as

$$K^{\text{eff}} = \frac{c^{(0)} K^{(0)} + \sum_{r=1}^n c^{(r)} K^{(r)} \left[1 + \alpha_0 \left(\frac{K^{(r)}}{K^{(0)}} - 1 \right) \right]^{-1}}{c^{(0)} + \sum_{r=1}^n c^{(r)} \left[1 + \alpha_0 \left(\frac{K^{(r)}}{K^{(0)}} - 1 \right) \right]^{-1}} \quad (3.59)$$

and the effective shear modulus as

$$G^{\text{eff}} = \frac{c^{(0)} G^{(0)} + \sum_{r=1}^n c^{(r)} G^{(r)} \left[1 + \beta_0 \left(\frac{G^{(r)}}{G^{(0)}} - 1 \right) \right]^{-1}}{c^{(0)} + \sum_{r=1}^n c^{(r)} \left[1 + \beta_0 \left(\frac{G^{(r)}}{G^{(0)}} - 1 \right) \right]^{-1}} \quad (3.60)$$

where

$$\alpha^{(0)} = \frac{3K^{(0)}}{3K^{(0)} + 4G^{(0)}} \quad \text{and} \quad \beta^{(0)} = \frac{6(K^{(0)} + 2G^{(0)})}{5(3K^{(0)} + 4G^{(0)})} \quad (3.61)$$

The Mori-Tanaka theories are based on the assumption that the shape of the inhomogeneities can be described by ellipsoids. In porous or cellular materials with high void volume fractions, the deformation at the microscale takes place due to bending and buckling of the cell walls (Gibson and Ashby, 1988), which implies changes of shapes of the voids. Such effects are not described by Mori-Tanaka models, which, consequently, tend to overestimate the effective stiffness of the cellular materials by far [5].

4 Strength Homogenization

Due to the assumed elastic linear behavior of the RVE, all the imposed work is stored at each point as an elastic energy density:

$$W_e = \frac{1}{2} \boldsymbol{\sigma} : \boldsymbol{\varepsilon} = \frac{1}{2} \boldsymbol{\varepsilon} : \mathbf{L} : \boldsymbol{\varepsilon} = \frac{1}{2} \boldsymbol{\sigma} : \mathbf{M} : \boldsymbol{\sigma} \quad (4.01)$$

which can be decomposed in the volumetric and deviatoric part as follows:

$$W_e = \frac{1}{2} \sigma_m \varepsilon_V + \frac{1}{2} \mathbf{s} : \mathbf{e} = W_{eV} + W_{eD} \quad (4.02)$$

where the deviatoric part

$$W_{eD} = \frac{1}{2} \mathbf{s} : \mathbf{e} = \frac{1}{4G} \mathbf{s} : \mathbf{s} \quad (4.03)$$

is assumed to cause the failure and it is proportional to so called second invariant of the stress deviator, J_2 , where:

$$J_2 = \frac{1}{2} s_{ij} s_{ij} \quad \text{and then} \quad W_{eD} = 2G J_2(\boldsymbol{\sigma}) \quad (4.04)$$

The invariant J_2 can be written using the Mandel notation as

$$J_2 = \frac{1}{2} \mathbf{s}^T \mathbf{s} \quad (4.05)$$

4.1 Quadratic Strain Averages

The expression for the quadratic average of the deviatoric strain field over a general phase r can be derived using the Hill's lemma

$$\langle U \rangle = \left\langle \frac{1}{2} E_{ij}^{(r)} L_{ijkl} E_{kl}^{(r)} \right\rangle = \frac{1}{2} \langle E_{ij}^{(r)} \rangle L_{ijkl}^{eff} \langle E_{kl}^{(r)} \rangle = \frac{1}{2} E_{ij} L_{ijkl}^{eff} E_{kl} \quad (4.06)$$

expressing the equality between the average strain energy density $\langle U \rangle$ in the RVE when expressed by means of the microscopic or macroscopic quantities [4] the following equation is obtained:

$$\mathbf{E} : \mathbf{L}^{eff} : \mathbf{E} = \frac{1}{|\Omega|} \int_{\Omega} \boldsymbol{\varepsilon}(\mathbf{x}) : \mathbf{L}(\mathbf{x}) : \boldsymbol{\varepsilon}(\mathbf{x}) d\mathbf{x} \quad (4.07)$$

The local strain $\boldsymbol{\varepsilon}(\mathbf{x})$ can be then decomposed into its volumetric and deviatoric part (causing the failure):

$$\mathbf{E} : \mathbf{L}^{eff} : \mathbf{E} = \frac{1}{|\Omega|} \int_{\Omega} \boldsymbol{\varepsilon}(\mathbf{x}) : [3K(\mathbf{x})\mathbf{I}_V + 2G(\mathbf{x})\mathbf{I}_D] : \boldsymbol{\varepsilon}(\mathbf{x}) d\mathbf{x} \quad (4.08)$$

which can be after projection of strain in each phase into its volumetric and deviatoric part written as

$$\mathbf{E} : \mathbf{L}^{eff} : \mathbf{E} = \frac{1}{|\Omega|} \sum_{r=0}^n \int_{\Omega^{(r)}} 3K^{(r)} \boldsymbol{\varepsilon}_V^{(r)} \boldsymbol{\varepsilon}_V^{(r)} + 2G^{(r)} \boldsymbol{\varepsilon}_{dev}^{(r)}(\mathbf{x}) : \boldsymbol{\varepsilon}_{dev}^{(r)}(\mathbf{x}) d\mathbf{x} \quad (4.09)$$

To extract the deviatoric part from the expression it is convenient to differentiate the whole equation with respect to $G^{(r)}$. The volumetric part after the differentiation vanishes and we obtain

$$\mathbf{E} : \frac{\partial \mathbf{L}^{eff}}{\partial G^{(r)}} : \mathbf{E} = \frac{1}{|\Omega|} \sum_{r=0}^n \int_{\Omega^{(r)}} 2\boldsymbol{\varepsilon}_{dev}^{(r)}(\mathbf{x}) : \boldsymbol{\varepsilon}_{dev}^{(r)}(\mathbf{x}) d\mathbf{x} \quad (4.10)$$

and after a simple manipulation

$$\frac{1}{2} \mathbf{E} : \frac{\partial \mathbf{L}^{eff}}{\partial G^{(r)}} : \mathbf{E} = \frac{1}{|\Omega|} \frac{|\Omega^{(r)}|}{|\Omega^{(r)}|} \sum_{r=0}^n \int_{\Omega^{(r)}} \boldsymbol{\varepsilon}_{dev}^{(r)}(\mathbf{x}) : \boldsymbol{\varepsilon}_{dev}^{(r)}(\mathbf{x}) d\mathbf{x} \quad (4.11)$$

the equation can be even more simplified as follows

$$\frac{1}{2} \mathbf{E} : \frac{\partial \mathbf{L}^{eff}}{\partial G^{(r)}} : \mathbf{E} = c^{(r)} \frac{1}{|\Omega^{(r)}|} \int_{\Omega^{(r)}} \boldsymbol{\varepsilon}_{dev}^{(r)}(\mathbf{x}) : \boldsymbol{\varepsilon}_{dev}^{(r)}(\mathbf{x}) d\mathbf{x} \quad (4.12)$$

The quadratic average of the deviatoric strain field over a general phase r is defined as [1]

$$\overline{\boldsymbol{\varepsilon}_{dev}^{(r)}} = \sqrt{\frac{1}{|\Omega^{(r)}|} \int_{\Omega^{(r)}} \frac{1}{2} \boldsymbol{\varepsilon}_{dev}^{(r)}(\mathbf{x}) : \boldsymbol{\varepsilon}_{dev}^{(r)}(\mathbf{x}) d\mathbf{x}} \quad (4.13)$$

and using the previous equations it can be also expressed as

$$\overline{\boldsymbol{\varepsilon}_{dev}^{(r)}} = \sqrt{\frac{1}{4c^{(r)}} \mathbf{E} : \frac{\partial \mathbf{L}^{eff}}{\partial G^{(r)}} : \mathbf{E}} \quad (4.14)$$

The related quadratic average of the deviatoric stress field (see the expression for J_2) is used as an estimate for deviatoric stress peaks [1]:

$$\overline{\sigma_{\text{dev}}^{(r)}} = \sqrt{\frac{1}{|\Omega^{(r)}|} \int_{\Omega^{(r)}} \frac{1}{2} \mathbf{s}_{\text{dev}}^{(r)}(\mathbf{x}) : \mathbf{s}_{\text{dev}}^{(r)}(\mathbf{x}) d\mathbf{x}} = 2 G^{(r)} \overline{\boldsymbol{\epsilon}_{\text{dev}}^{(r)}} \quad (4.15)$$

where $\mathbf{s}(\mathbf{x})$ denotes the field of the deviatoric stress tensor.

Assuming the elasto-brittle approach, the elastic behavior prevails until the quadratic deviatoric stress averages over each of the phases remain below a critical strength [1]:

$$\overline{\sigma_{\text{dev}}^{(r)}} \leq \sigma_{\text{dev,crit}}^{(r)} \quad (4.16)$$

5 Homogenization with Coated Particles

This section is devoted to the evaluation of the constraint constants for coated particles, relating the induced strain to the eigenstrain in individual phases, $a^{(r)}$ and $\beta^{(r)}$, and obtaining the effective elastic properties. The spherical inclusion, with a thin interlayer, embedded in matrix is considered for the evaluation. This is an enormous simplification and it is also a good model for randomly oriented inhomogeneities, such as particles embedded in the mortar paste. Only the formulas needed for the derivation of $a^{(r)}$ and $\beta^{(r)}$ are provided in this thesis, the theoretical background can be found in [16].

Motivated by Eshelby's observations, Luo and Weng [16] undertook a similar study to find the elastic field in the inclusion (grain) and coating, which is embedded in an infinitely extended matrix. They restricted their consideration to the case of a three-phase, spherically concentric solid.

The whole procedure for determination of the constraint constants, $a^{(g)}$ and $\beta^{(g)}$ representing the grain, $a^{(c)}$ and $\beta^{(c)}$ representing the coating and finally $a^{(m)}$ and $\beta^{(m)}$ representing the matrix, was taken from [16]. All the phases, grain, coating and matrix, are represented by bulk modulus $K^{(r)}$ and shear modulus $G^{(r)}$. The geometry is described by the radius of a grain a and radius of its coating b , as depicted in the following figure:

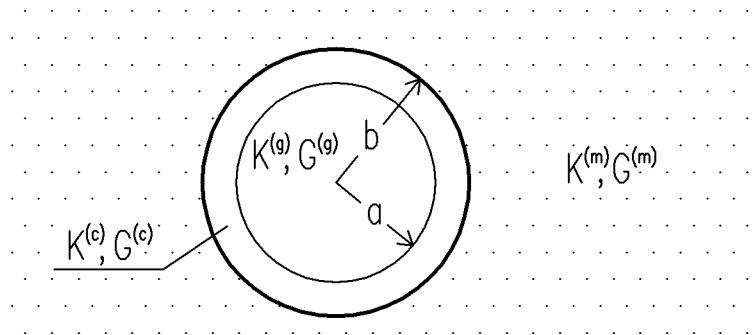


Fig. 5.1: A three-phase composite spherically concentric solid

The superscript g stands for the grain (or the inner inclusion), c stands for the coating and superscript m is used in quantities describing the surrounding matrix.

The parameter c is defined as $c = (a / b)^3$ and it has a physical meaning of the volume fraction of particles in a two-phase composite. The hydrostatic and deviatoric transformation problems are treated separately.

The solution of Luo and Weng is based on the equation for the general displacement field in spherical coordinates. The integration constants are found using the continuity conditions and equilibrium of stresses on the interface of individual phases.

5.1 Hydrostatic Part

A theoretical background for obtaining the following formulas can be found in [16] from which only the needed expressions for constraint constants are presented here. The constraint constant for grain $a^{(g)}$ is calculated as

$$\alpha^{(g)} = 3K^{(g)} \left[(3K^{(c)} + 4G^{(m)}) - 4c(G^{(m)} - G^{(c)}) \right] / p \quad (5.01)$$

where c was defined as $c = (a/b)^3$ and p is

$$p = (3K^{(g)} + 4G^{(c)})(3K^{(c)} + 4G^{(m)}) - 12c(K^{(g)} - K^{(c)})(G^{(m)} - G^{(c)}) \quad (5.02)$$

The constrain constant for the coating of a grain is obtained as

$$\alpha^{(c)} = -4cK^{(g)}(G^{(m)} - G^{(c)}) / p \quad (5.03)$$

5.2 Deviatoric Part

As in case of the hydrostatic constraint constants $a^{(r)}$, the derivation of the expressions for the deviatoric constraint constants $\beta^{(r)}$ is, together with a theoretical background, provided in [16]. Again, only the needed formulas are presented here.

The deviatoric constraint constant for the grain can be found in the form

$$\beta^{(g)} = a_1 - \frac{21}{5(1-\nu^{(g)})} a_2 \quad (5.04)$$

and for the coating as

$$\beta^{(c)} = b_1 - \frac{21}{5(1-2\nu^{(c)})} \frac{1-c^{5/3}}{1-c} b_2 \quad (5.05)$$

where the constants a_1 and a_2 can be calculated as

$$\begin{pmatrix} a_1 \\ a_2 \end{pmatrix} = \mathbf{R}^{-1} \quad (5.06)$$

and the terms b_1 and b_2 , needed for the calculation of the deviatoric constraint constants of coating, can be found as

$$\begin{pmatrix} b_1 \\ b_2 \\ b_3 \\ b_4 \end{pmatrix} = \mathbf{E}^{-1} \mathbf{F} \mathbf{K}^{-1} \mathbf{H} \mathbf{R}^{-1} \quad (5.07)$$

The individual matrices needed in the previous equations can be obtained as

$$\mathbf{E} = \begin{bmatrix} 1 & -\frac{6\nu^{(c)}}{1-2\nu^{(c)}} & 3 & \frac{5-4\nu^{(c)}}{1-2\nu^{(c)}} \\ 1 & -\frac{7-4\nu^{(c)}}{1-2\nu^{(c)}} & -2 & 2 \\ 1 & \frac{3\nu^{(c)}}{1-2\nu^{(c)}} & -12 & \frac{-2(5-\nu^{(c)})}{1-2\nu^{(c)}} \\ 1 & -\frac{7+2\nu^{(c)}}{1-2\nu^{(c)}} & 8 & \frac{2(1+\nu^{(c)})}{1-2\nu^{(c)}} \end{bmatrix} \quad (5.08)$$

$$\mathbf{F} = \begin{bmatrix} 3 & \frac{5-4\nu^{(m)}}{1-2\nu^{(m)}} \\ -\frac{2}{12G^{(m)}} & \frac{-2(5-\nu^{(m)})}{1-2\nu^{(m)}} \frac{G^{(m)}}{G^{(c)}} \\ \frac{8G^{(m)}}{G^{(c)}} & \frac{2(1+\nu^{(m)})}{1-2\nu^{(m)}} \frac{G^{(m)}}{G^{(c)}} \end{bmatrix} \quad (5.09)$$

$$\mathbf{H} = \begin{bmatrix} 1 & -\frac{6\nu^{(g)}}{1-2\nu^{(g)}} \\ 1 & -\frac{7-4\nu^{(g)}}{1-2\nu^{(g)}} \end{bmatrix} \quad (5.10)$$

$$\mathbf{K} = \mathbf{G} \mathbf{E}^{-1} \mathbf{F} \quad (5.11)$$

$$\mathbf{R} = \mathbf{P} + \mathbf{Q} \mathbf{E}^{-1} \mathbf{F} \mathbf{K}^{-1} \mathbf{H} \quad (5.12)$$

where

$$\mathbf{G} = \begin{bmatrix} 1 & -\frac{6\nu^{(c)}c^{2/3}}{1-2\nu^{(c)}} & \frac{3}{c^{5/3}} & \frac{5-4\nu^{(c)}}{(1-2\nu^{(c)})c} \\ 1 & -\frac{(7-4\nu^{(c)})c^{2/3}}{1-2\nu^{(c)}} & -\frac{2}{c^{5/3}} & \frac{2}{c} \end{bmatrix} \quad (5.13)$$

$$\mathbf{P} = \begin{bmatrix} 1 & \frac{3\nu^{(g)}}{1-2\nu^{(g)}} \\ 1 & -\frac{7+2\nu^{(g)}}{1-2\nu^{(g)}} \end{bmatrix} \quad (5.14)$$

and finally

$$\mathbf{Q} = \frac{G^{(c)}}{G^{(g)}} \begin{bmatrix} -1 & -\frac{3\nu^{(c)}c^{2/3}}{1-2\nu^{(c)}} & \frac{12}{c^{5/3}} & \frac{2(5-\nu^{(c)})}{(1-2\nu^{(c)})c} \\ -1 & \frac{(7+2\nu^{(c)})c^{2/3}}{1-2\nu^{(c)}} & -\frac{8}{c^{5/3}} & -\frac{2(1+\nu^{(c)})}{(1-2\nu^{(c)})c} \end{bmatrix} \quad (5.15)$$

5.3 Modification of Mori-Tanaka Homogenization

For the calculation of the effective moduli, the formulas for spherical inclusions developed in the chapter 3 can be used in a slightly modified form. The effective bulk modulus can be expressed, according to Mori-Tanaka scheme, as

$$K^{eff} = \frac{c^{(0)}K^{(0)} + \sum_{r=1}^n c^{(r)}K^{(r)} \left[1 + \alpha^{(r)} \left(\frac{K^{(r)}}{K^{(0)}} - 1 \right) \right]^{-1}}{c^{(0)} + \sum_{r=1}^n c^{(r)} \left[1 + \alpha^{(r)} \left(\frac{K^{(r)}}{K^{(0)}} - 1 \right) \right]^{-1}} \quad (5.16)$$

and the effective shear modulus as

$$G^{eff} = \frac{c^{(0)}G^{(0)} + \sum_{r=1}^n c^{(r)}G^{(r)} \left[1 + \beta^{(r)} \left(\frac{G^{(r)}}{G^{(0)}} - 1 \right) \right]^{-1}}{c^{(0)} + \sum_{r=1}^n c^{(r)} \left[1 + \beta^{(r)} \left(\frac{G^{(r)}}{G^{(0)}} - 1 \right) \right]^{-1}} \quad (5.17)$$

where the constraint constants $a^{(r)}$ and $\beta^{(r)}$ differ for the phases within the coated grain (inclusion) and those having no coating. For the grain and coating, the constraint constants presented in the previous sections of this chapter have to be used. In case of the particles without coating, the constraint constants $a^{(r)}$ and $\beta^{(r)}$ can be simply substituted by a_0 and β_0 , which are dependent only on the Poisson's ratio of the surrounding matrix, as defined in the chapter 3.

PART II:
CALCULATIONS

6 Introduction to Cocciopesto Mortars

Air lime based mortars harden through drying and carbonation of so-called slaked lime, Ca(OH)_2 , that transforms into calcite, CaCO_3 , in presence of atmospheric CO_2 . In hydraulic mortars, this hardening is supplemented by chemical reactions between calcium hydroxide and reactive silicates and aluminates in the presence of water. These minerals are not present in limestone in the sufficient quantities and therefore they must be added in form of pozzolans.

Hydraulic limes have more favorable properties, mainly higher strength [6]. The term 'hydraulic' is now used internationally to describe cements and other binders, which set and harden as a result of chemical reactions with water and continue to harden even if subsequently placed under water [7].

Pozzolans are able to react with the calcium hydroxide at ambient temperature to form hydrated calcium silicates and develop suitable mechanical strengths. In fact, the pozzolan-lime reaction is also a hydraulic reaction which main hydration product is C-S-H gel, like in Portland cement [6].

The use of mortars based on hydrated lime and brick dust dates back to the most ancient times. Phoenicians were probably the first ones to use mortars based on hydrated lime and crushed or dust bricks, followed by all other people who were in contact with them. The Romans used this type of mortar in every part of their empires whenever pozzolanic materials were not available and a mortar insoluble in water was needed. They certainly were ignorant of the chemistry of mortars, but they knew by experience that the brick dust or pebble played a very important role in the mortar consistency and strength. The use of crushed bricks, particularly brick dust, in the preparation of mortars based on putty lime has been interpreted in the present time as an alternative use to other pozzolanic materials [9].

The specific hydraulic character of the crushed brick-lime mortar is attributed to the adhesion reactions occurring at the ceramic-matrix interface, on the calcium hydrate content of the mortar and the dimensions and type of ceramic [8].



Fig. 6.1: *Hagia Sophia mortar sample* [12]

Reactions between the lime and any pozzolanic material take place if the pozzolanic material is finely ground in order to make a large, specific surface, and hence a large contact between the two materials. When the joint thickness becomes greater than 40 mm (70 mm in case of Hagia Sophia in Istanbul), the size of the brick pebbles increases even up to 25 mm and the pozzolanic reaction, if any, can take place only along the external border of the pebble [9].

Clay minerals in the clay bricks, composed mainly of silica and alumina, present a sharp pozzolanic activity when heated at temperatures in the range of 600–900°C and ground in sufficient fineness. During the thermal treatment, silica and alumina lose the combined water, leading to a destruction of the crystalline network. Silica and alumina remain in an unstable amorphous phases that could react with hydrated lime and water, producing pozzolanic products [10].

The lime makes the interfacial surface alkaline and causes chemical reaction. The penetration of lime into the ceramic and the consequent reaction, transform the microstructure of the ceramic by reduction of pore radii [8].

Mortar samples also show self-healing effects and proved to be resistant to continuous stresses and strains due to the above-mentioned presence of the amorphous hydraulic formations (C-S-H) which allows for greater energy absorption without initiations of fractures and explains the good performance of the historic composites [11], [12].

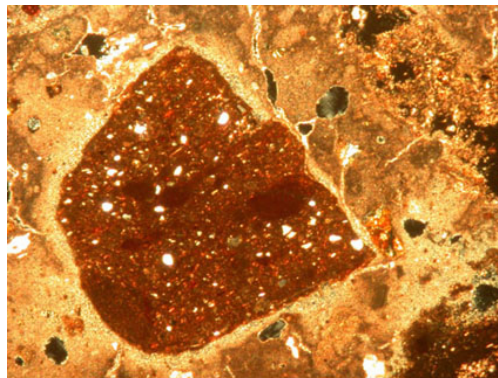


Fig. 6.2: Fragment of pottery in cocchiopesto with thin layer of C-S-H [15]

Based on the literature study, it seems that no one has ever tried to estimate the properties of cocchiopesto mortars using micromechanical modeling. Two works [1] and [27] provided an inspiration for developing micromechanical models. These works deal with composite materials, composed of the matrix, voids and aggregates and exploit the method of Mori-Tanaka (Mori and Tanaka, 1973) to estimate the effective stiffness and strength of the composite. Even though there are many simplifications in these models, the results quite well correspond to the available experimental data and therefore they should be applicable to the mortars with crushed bricks as well.

7 Calculation without C-S-H Gel Coating

Based on a comprehensive literature study, e.g. [22], the mix proportions for the micromechanical homogenization of the cocciopesto mortar were determined as 4 mass portions of lime matrix, 3 mass portions of crushed bricks, or other clay products such as ceramic tiles, and 5 mass portions of siliceous sand in the hardened mortar.

This composition should be similar to the historic mortars described by, for instance, Vitruvius. The crushed bricks should be responsible for the hydraulicity, and therefore improve the mechanical properties of the mortar, without need for the modern artificial substances or industrial by-products such as metakaolin or fly ash.

Table 7.1: properties of individual components used for calculation

	density	Young's modulus	Poisson's ratio	tensile strength	source
	kg/m ³	MPa	-	MPa	-
lime	1 900	1 800	0.25	0.4	[24]
siliceous sand	2 600	70 000	0.17	48	[25]
clay brick	1 600	2 400	0.17	3.2	[23]
voids	-	0.001	0.001	-	-

The porosity of hardened mortar is varying according to the environment and technology. For the calculations, the porosity was considered to be 30% of the volume, if not specified otherwise.

The mechanical properties of the individual components, considered in the calculations, are summarized in Table 7.1. The properties of voids are set to be non-zero to avoid any complications during the computations.

The summary of material properties in Table 7.1 indicates that the “weak” constituent is the hardened lime matrix, having the tensile strength approximately 0.4 MPa. This value can vary according to curing time and technology. However, the value should not be higher than 0.7 MPa, which is still way smaller than the tensile strength of the other components.

For the calculation of the effective (overall, macroscopic) material properties, the Mori-Tanaka homogenization technique was used. The representation of randomly oriented inhomogeneities by spherical particles was chosen, since these should demonstrate the trends in behavior as the best ones.

All the calculations presented in this work were done using software MATLAB.

7.1 Calculation of Effective Stiffness without C-S-H Gel Formation

The final stiffness (Young's modulus) of the mix is strongly influenced by the porosity of the hardened mortar. For illustration see the following figure, where the dependence of the mortar stiffness and Poisson's ratio on the porosity is depicted:

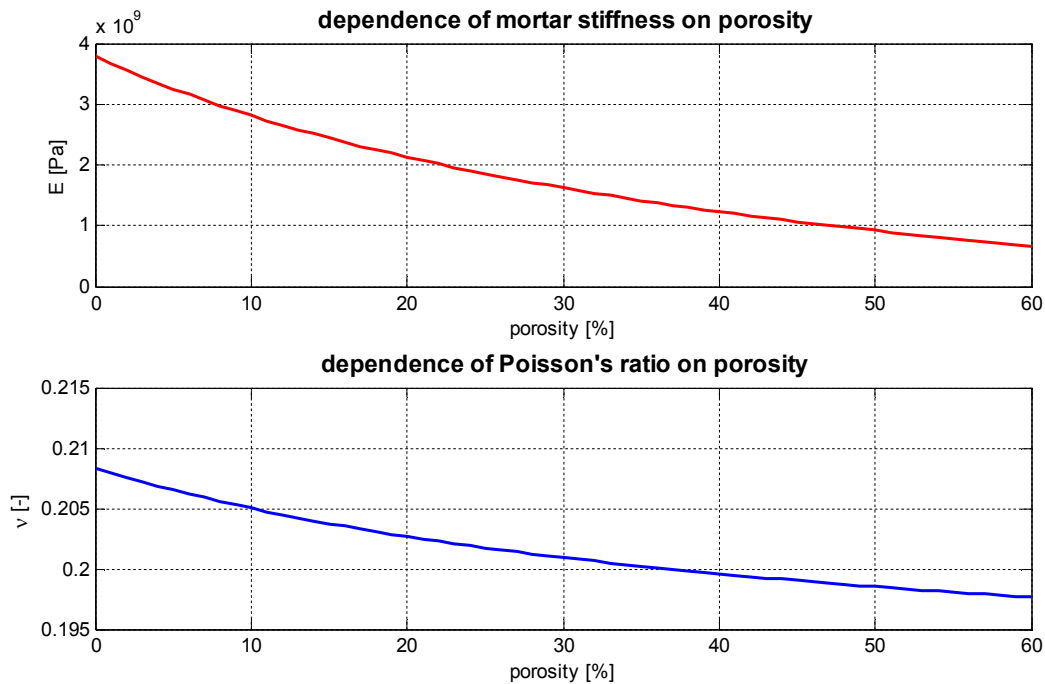


Fig. 7.2: Dependence of effective stiffness and Poisson's ratio on porosity of mortar

For the reasonable porosity of 30%, the calculated Young's modulus of the mortar is $E^{eff} = 1\,621$ MPa and Poisson's ratio $\nu^{eff} = 0.201$. These values yield the effective shear modulus of the mortar $G^{eff} = 675$ MPa.

The calculated effective stiffness is within the range provided in literature. The stiffness of historic cocciopesto mortars varies according to their porosity and content of the individual constituents - the values of Young's modulus can be lower than 1 000 MPa (e.g. [13]) and also higher than 3 000 MPa, corresponding to the stiff cocciopesto mortars with high pozzolanicity and low porosity (e.g. [14]).

The stiffness of the mix is decreasing with the increasing content of crushed bricks. The variable parameter a (brick content) has a meaning of the mass portion in the mix (lime : brick : sand = 4 : a : 5). The calculated trend is shown in the following figure:

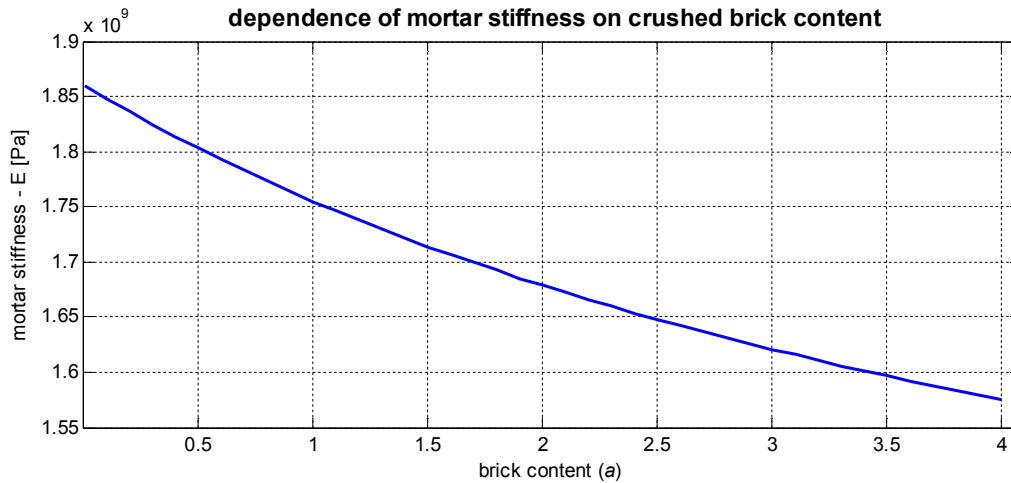


Fig. 7.3: Dependence of macroscopic mortar stiffness on content of crushed bricks

7.2 Estimation of Strength without C-S-H Gel Formation

The quadratic average of the deviatoric stress within the weakest phase (lime matrix) was estimated in order to determine the effect of crushed bricks in the cocciopesto mortar. Such approach was inspired by estimation of the compressive strength of a cement paste and mortar by [1].

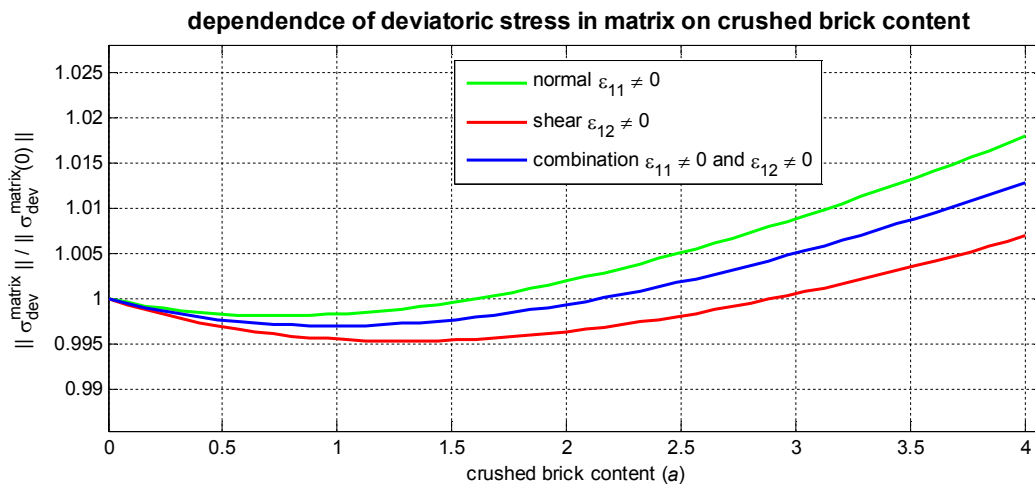


Fig. 7.4: Dependence of quadratic average of deviatoric stress in mortar on content of crushed bricks

First, the constant macroscopic strains (unit normal strain ϵ_{11} and unit shear strain ϵ_{12}) were assumed as loading parameters. By addition of the crushed clay bricks in a reasonable amount into the mix the deviatoric stress within the mortar phase decreased. It should make the lime matrix less vulnerable to damage. The dependence of the quadratic deviatoric stress average within the matrix phase on the

brick content is depicted in the Fig. 7.4. The value of the deviatoric stress within the matrix, dependent on the brick content a , is divided by a reference value – the deviatoric stress within the matrix for the brick content $a = 0$, denoted as $\sigma_{\text{dev}}^{\text{matrix}}(0)$.

The stiffness of bricks has also its influence – Fig. 7.5 shows the dependence of the ratio $\|\sigma_{\text{dev}}^{\text{matrix}}(a)\| / \|\sigma_{\text{dev}}^{\text{matrix}}(0)\|$ on the brick content a for different stiffness of bricks. The values of elastic moduli E^{brick} are not realistic and are used only to indicate the trend:

dependence of deviatoric stress in matrix on crushed brick content loaded by $\sigma_{11} \neq 0$ and $\sigma_{12} \neq 0$

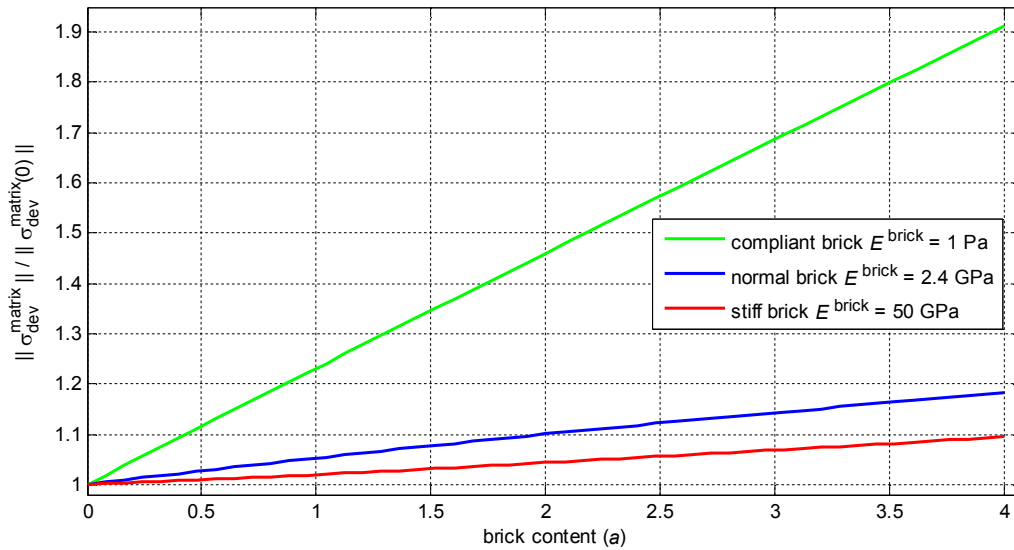


Fig. 7.5: Dependence of quadratic average of deviatoric stress in mortar on content of crushed bricks for different brick stiffness

The sample was loaded by a combination of normal and shear stress. This loading was chosen since it should be the critical one and it should simulate the loading induced during earthquake, to which the cocciopesto mortars should resist better than conventional mortars based on lime.

It can be seen in Fig. 7.5 that the more compliant bricks are added, the more deviatoric stress in the matrix phase can be expected. Also, the addition of voids, as the most compliant phase, increases the deviatoric stress in the matrix.

Due to the nature of the formulas used in homogenization according to the Mori-Tanaka scheme, it turns out that the rate of relief, $\|\sigma_{\text{dev}}^{\text{matrix}}(a)\| / \|\sigma_{\text{dev}}^{\text{matrix}}(0)\|$, in the individual phases is the same for all inclusions and inhomogeneities embedded in the matrix. In the case of cocciopesto mortar, the estimated increase of deviatoric stress in the matrix, sand and brick particles with an increasing porosity can be seen in Fig. 7.6.

dependence of deviatoric stress in individual phases on crushed brick content if loaded by $\sigma_{11} \neq 0$ and σ_{12}

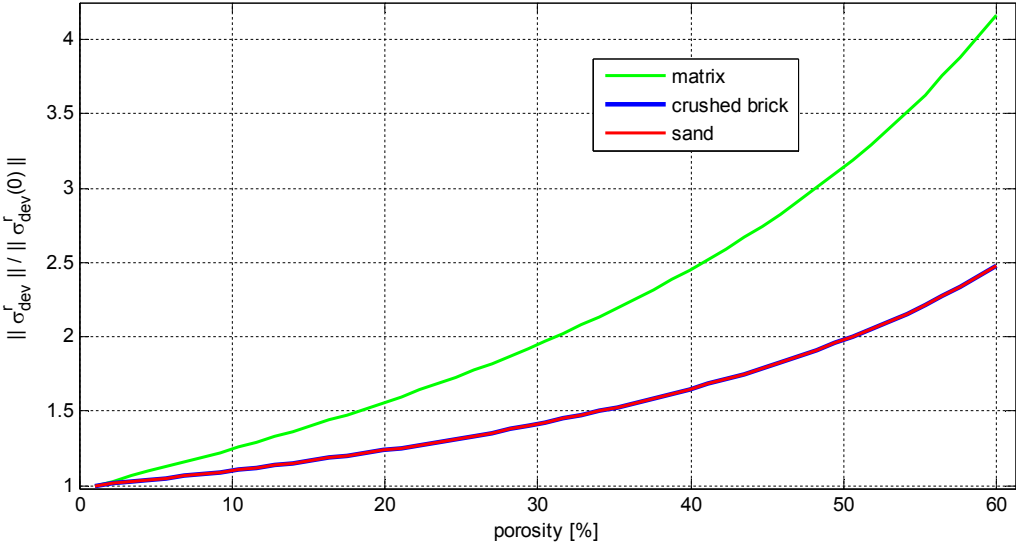


Fig. 7.6: Dependence of quadratic average of deviatoric stress in individual phases on porosity

8 Calculation with C-S-H Gel Coating

It is reported in many papers, dealing with the cocciopesto mortars, that the thin layer of C-S-H gel forms at the lime - brick interface if the bricks are made of clay and are burnt at the appropriate firing temperature (which is about 600–900°C [21]). The C-S-H gel is an amorphous phase with properties, responsible for some extraordinary properties of Portland cement concrete.

The thickness of the C-S-H layer at the brick interface is assumed to be about 20 μm for the calculations; the backscattered electron image of the interface can be seen in the following figure [17]:

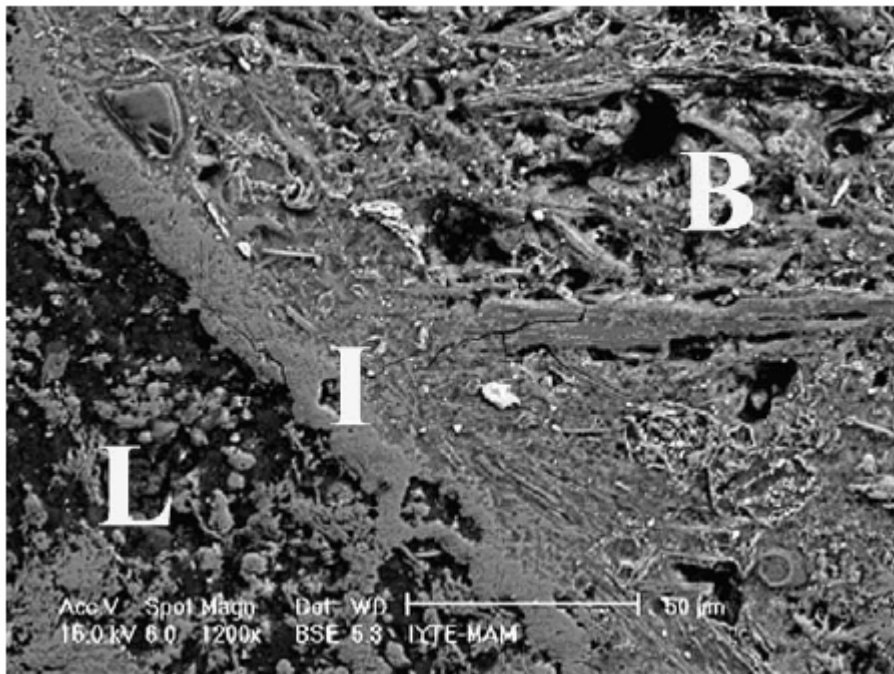


Fig. 8.1: Brick interface (I) between lime matrix (L) and brick aggregate (B) [17]

The estimation of the C-S-H gel thickness on the brick interface is one of the deficiencies in the modeling, however the thickness of 20 μm should be in a reasonable range. Another uncertainty is the elastic stiffness of the gel. There are basically two types of the gel present in Portland cement. As reported in the literature, e.g. [18], these are the low and high-density C-S-H gel. For the calculation of the effective properties of cocciopesto mortar, the properties of the low-density C-S-H gel were considered.

The nanoindentation results showed that the low-density C-S-H phase has a mean stiffness of about 22 GPa [19]. The density of the gel in calculation was considered as 2000 kg/m^3 , as suggested in [20] and Poisson's ratio as 0.20.

It is assumed in the calculations that 50% of the C-S-H gel occupies the voids, 30% of the C-S-H gel is assumed to consume the part of the matrix and the remaining 20%

is assumed to consume the part of the brick phase. These values are estimated, but they do not have any significant influence on the final results. Despite the uncertain material properties of the gel phase, the model is capable of predicting trends; however, it cannot predict the exact values.

For the coated inhomogeneities, the procedure suggested by [16], which is briefly described in this work (in the chapter 5), was used. As previously mentioned, the MATLAB software was used for all the calculations.

8.1 Calculation of Effective Stiffness with C-S-H Gel Formation

All the calculations presented in this chapter, if not specified otherwise, are done assuming the size of the brick particles as 1 mm in diameter. It was assumed that the C-S-H gel coating significantly stiffens the brick particles. This should result in an increase of the cocciopesto mortars stiffness if the coating is created, even if the layer is relatively thin in comparison with the diameter of the brick particles.

For the same composition of the mortar, the calculated Young's modulus of the mortar increased from $E^{eff} = 1\,621$ MPa to $E^{eff} = 1\,825$ MPa, if the formation of the C-S-H gel on the interface of brick particles was considered. The effect of the C-S-H coating on the effective stiffness of the mortar can be clearly seen in the following figure:

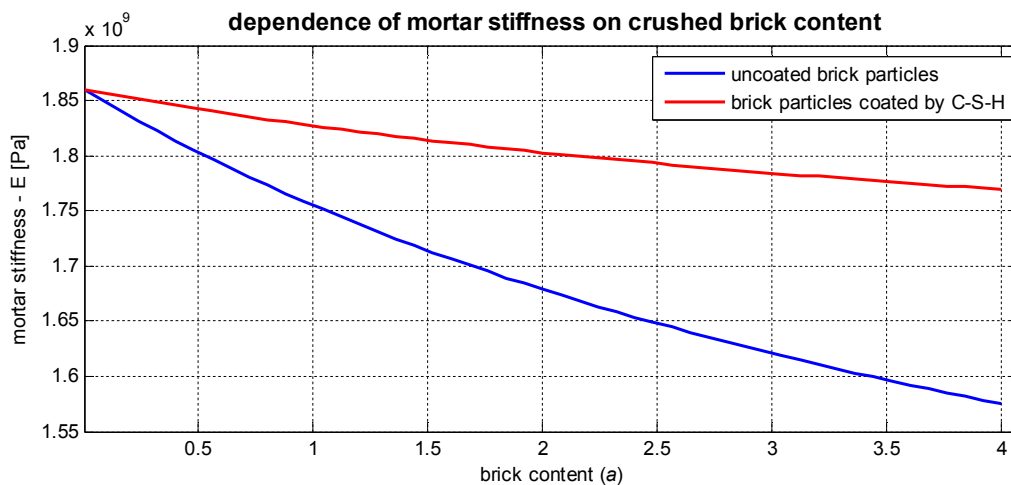


Fig. 8.2: Dependence of the effective stiffness on content of brick particles in mortar

The effective stiffness of mortar increases with a ratio of the coating thickness to the size of brick particles. It is indicated in the Fig. 8.3, where the dependence of the elastic stiffness on the thickness of the C-S-H gel coating is depicted:

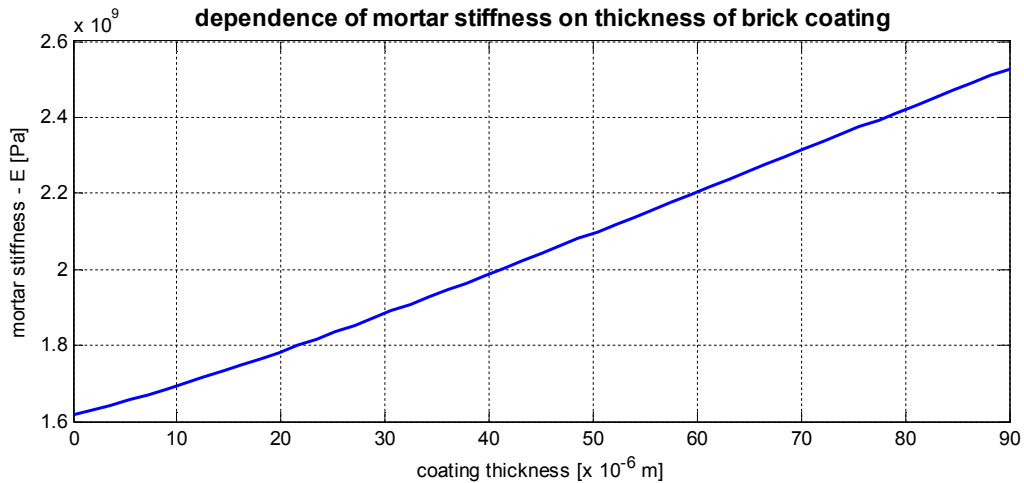


Fig. 8.3: Dependence of effective mortar stiffness on thickness of C-S-H gel coating

The ratio of the coating thickness to the size of brick particles also increases with the decreasing size of the brick particles. While the effective stiffness decreases with the addition of the crushed bricks of a big diameter (brick pebbles), the opposite is true for the tiny particles (brick dust). This can be seen in Fig. 8.4, showing the dependence of the effective stiffness on the brick content for relatively small and big crushed brick particles.

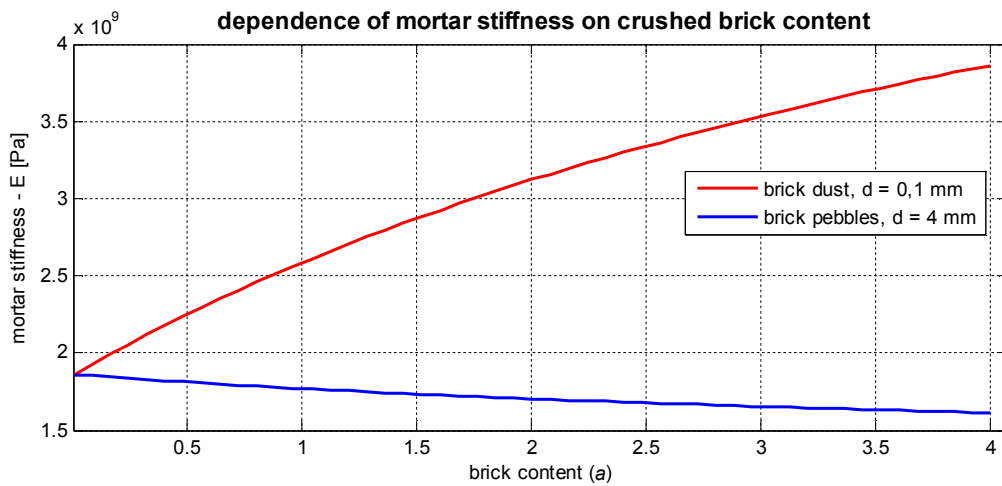


Fig. 8.4: Effective stiffness of mortar with coated and uncoated brick particles

It can be concluded that the C-S-H gel formation on the interface of the brick particles results in an increase of the effective stiffness of the mortar mix. This increase in stiffness is higher if the ratio of gel thickness to size of brick particles is relatively high. This can be ensured by the addition of the brick particles having smaller diameter.

8.2 Estimation of Strength with C-S-H Gel Formation

The estimation of strength, based on the calculation of the deviatoric stress average in the individual phases, was done as in case of mortar without C-S-H gel, according to the procedure used in [1].

The increase or reduction of the deviatoric stress in matrix is strongly dependent on the coating thickness to size of brick particles ratio. If the added crushed brick particles are smaller, the effect of C-S-H gel coating becomes greater and the deviatoric stress within the matrix phase significantly reduces. Therefore, it seems reasonable to add a certain amount of the finely crushed bricks into to the mix, since it should result in the decrease of the deviatoric stress within the matrix, as indicated in the following figure:

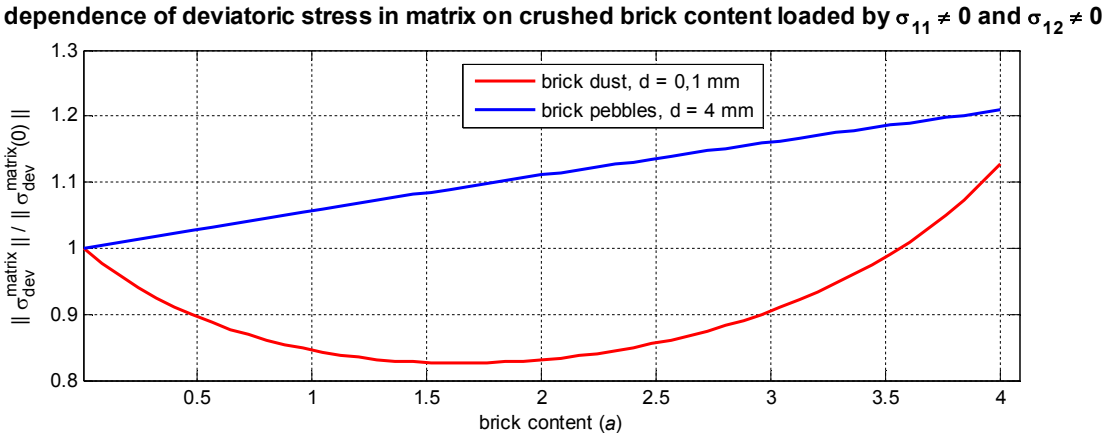


Fig. 8.5: Dependence of deviatoric stress in matrix for different size of brick particles

9 Calculation with Multiple Brick Fractions

If the C-S-H gel coating is formed, the addition of the crushed brick particles having a small diameter should result in an increase of the effective stiffness of the mortar mix, and decrease of the deviatoric stress within the matrix. These phenomena are shown in Fig. 9.1 and Fig. 9.2. The lime matrix to crushed bricks to sand ratio 4 : 3 : 5 in the hardened mortar, having the porosity of 30%, was used.

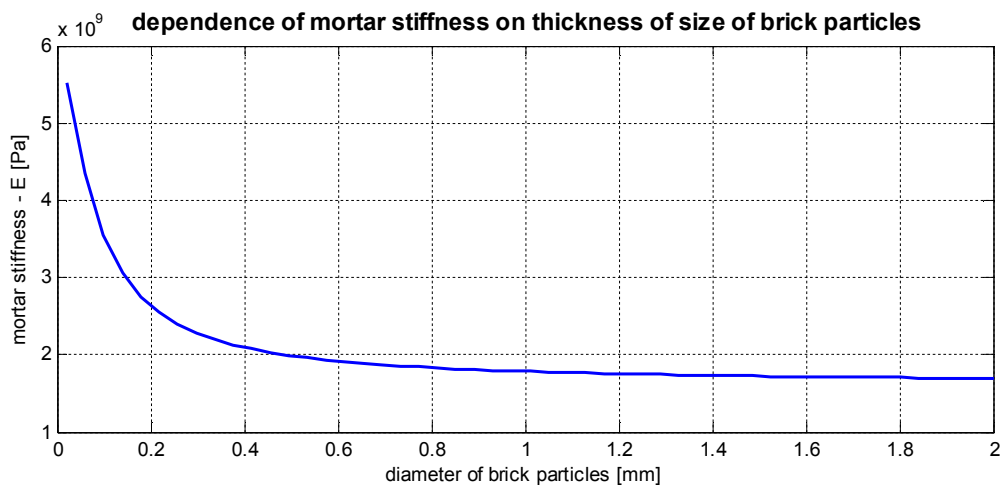


Fig. 9.1: Dependence of mortar stiffness on diameter of brick particles

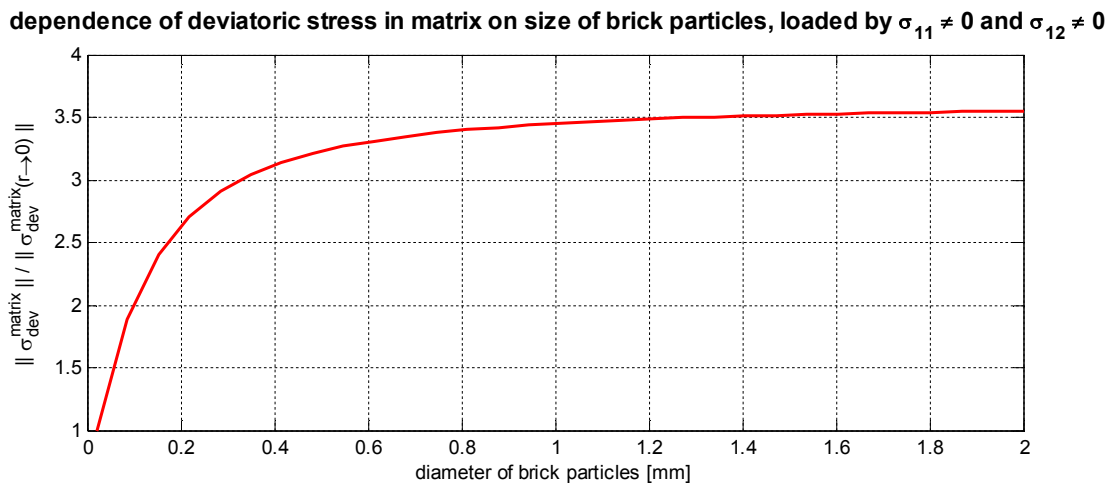


Fig. 9.2: Dependence of deviatoric stress increase in matrix on diameter of brick particles

For the conservation mortars a low elastic modulus and sufficient strength are, together with ductility, usually required [26]. The proper composition of the mortar can be prepared by using multiple fractions of crushed bricks. The fine brick particles in the mix should ensure the decrease of the deviatoric stress in matrix, and therefore

increase the mortar strength. On the other hand, the bigger fractions decrease the Young's modulus and make the mortar more compliant.

The graph in Fig. 9.3 shows the dependence of the deviatoric stresses ratio on the amount of fine brick fraction within the brick particles. The quantity $\|\sigma_{\text{dev}}^{\text{matrix}}\|$ stands for the deviatoric stress in matrix, corresponding to the given amount of fine brick particles substituting the big ones. $\|\sigma_{\text{dev}}^{\text{matrix}}(m=0)\|$ represents the deviatoric stress in the matrix if the mix does not contains any crushed bricks at all.

dependence of deviatoric stress in matrix on fraction of brick particles, loaded by $\sigma_{11} \neq 0$ and $\sigma_{12} \neq 0$

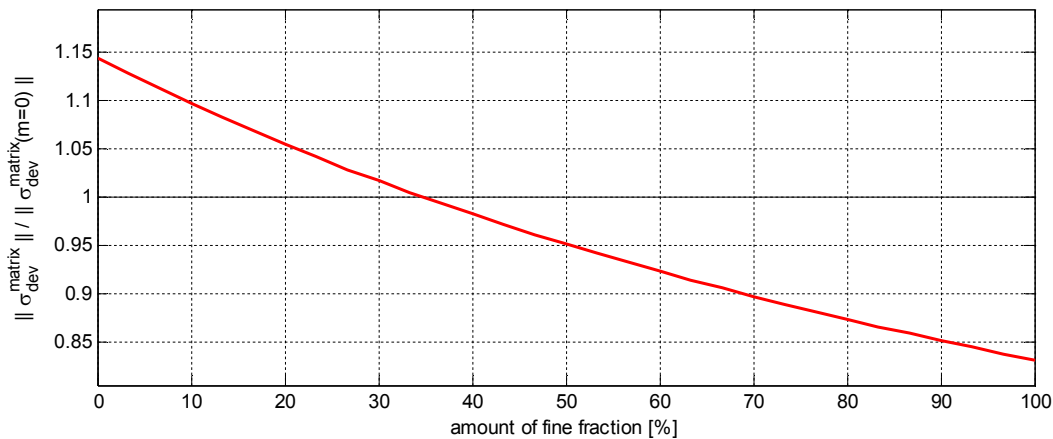


Fig. 9.3: Dependence of deviatoric stress in matrix on diameter of brick particles

It is clear from Fig. 9.3 that for the deviatoric stress decrease there should be more than 35 % of fine particles of crushed bricks (diameter 0.125 - 0.25 mm) and less than 65% of brick pebbles (diameter 2 - 4 mm) in the mix. However, the prevailing fine crushed brick fractions cause an increase of mortar stiffness (Fig. 9.4)

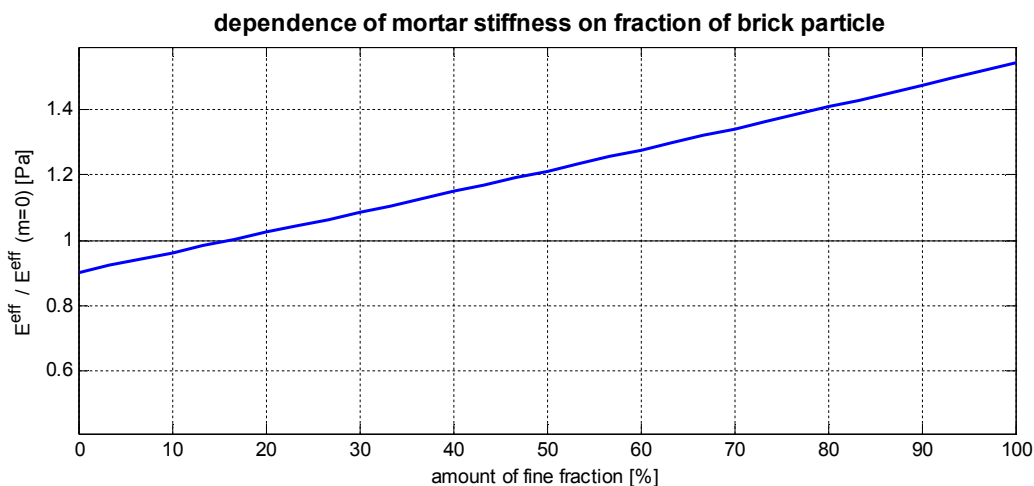


Fig. 9.4: Dependence of mortar stiffness on diameter of brick particles

It can be concluded from the previous figures that the reduction of the deviatoric stress in matrix is coupled with an increased effective stiffness.

9.1 Crushed Brick Size Optimization

A fraction of crushed bricks can be optimized towards a bigger compliance or bigger strength. This chapter provides an example of the crushed brick fractions optimization towards a better performance.

The mortar composition is considered, as previously, with the lime matrix to crushed bricks to sand ratio 4 : 3 : 5 in the hardened mortar, having the porosity of 30%. First, a crushed brick fractions used in historic mortar, found in a Byzantine ancient structure and investigated by [9], was considered in calculation. Then the amount of individual crushed brick fractions was modified in such a way that the effective stiffness of the mortar is not significantly increased and the deviatoric stress in matrix is reduced.

It should be noted that only the fractions of crushed bricks are corresponding to the mortar samples from the Byzantine structure described in [9], not the ratio of mortar constituents. In addition, the biggest fractions of crushed bricks, exceeding 4 mm were eliminated. However, the indicated trends should be valid for any similar mortar composition, based on lime, crushed bricks and sand, having a reasonable porosity.

It was found in [9] that the investigated Byzantine mortar had a crushed brick size distribution approximately as follows:

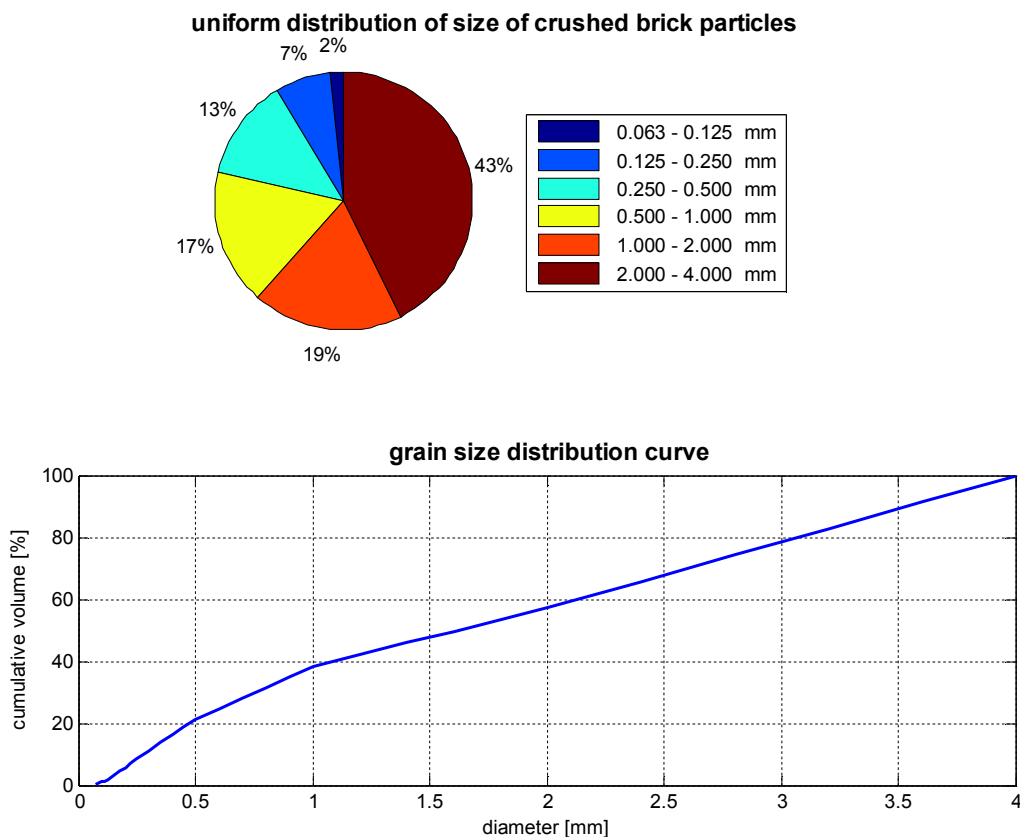


Fig. 9.5: Approximate distribution of crushed brick size in ancient Byzantine structure

Such distribution of crushed brick particles should, using the micromechanical approach and assuming the above mentioned mortar composition, yield the effective mortar stiffness $E^{\text{eff}} = 1909 \text{ MPa}$.

The modification of the brick particles distribution was focused on reduction of deviatoric stress in the matrix, while increasing the effective mortar stiffness as little as possible. The distribution of brick particles in the modified mortar can be seen in Fig. 9.6. The medium-size particles were eliminated and only the small particles, ensuring the decrease of deviatoric stress, were combined with particles of big size to ensure a relatively low increase of the effective mortar stiffness.

The fractions 0.063 – 0.125 and 0.125 – 0.250 mm in diameter were chosen to represent the small brick particles, because these fractions are reasonable with respect to the production possibilities. On the other hand, the fraction 2 – 4 mm representing the big particles can be substituted practically by any size of crushed bricks above 2 mm without influence on the results.

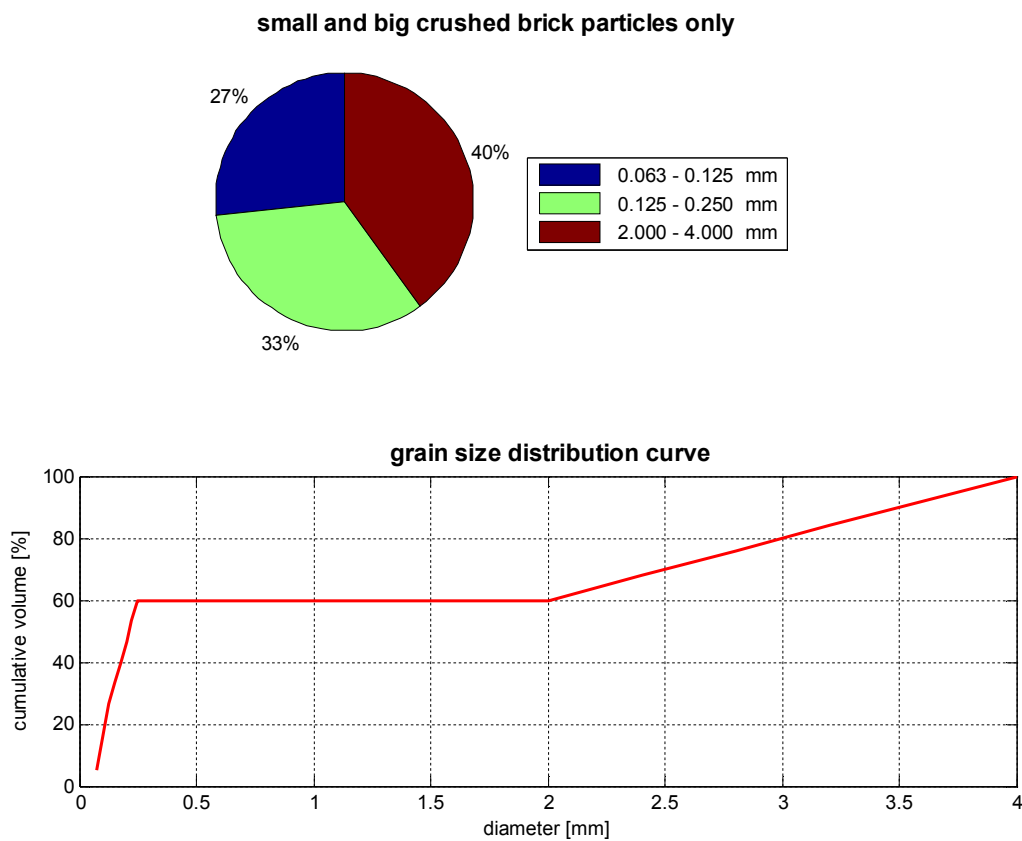


Fig. 9.6: Modified crushed brick size distribution

The calculated effective stiffness of mortar, having the modified distribution of crushed brick particles, is $E^{\text{eff}} = 2646 \text{ MPa}$. The dependence of the effective stiffness on brick content, considering the original and modified crushed brick size distribution, is depicted in the following figure:

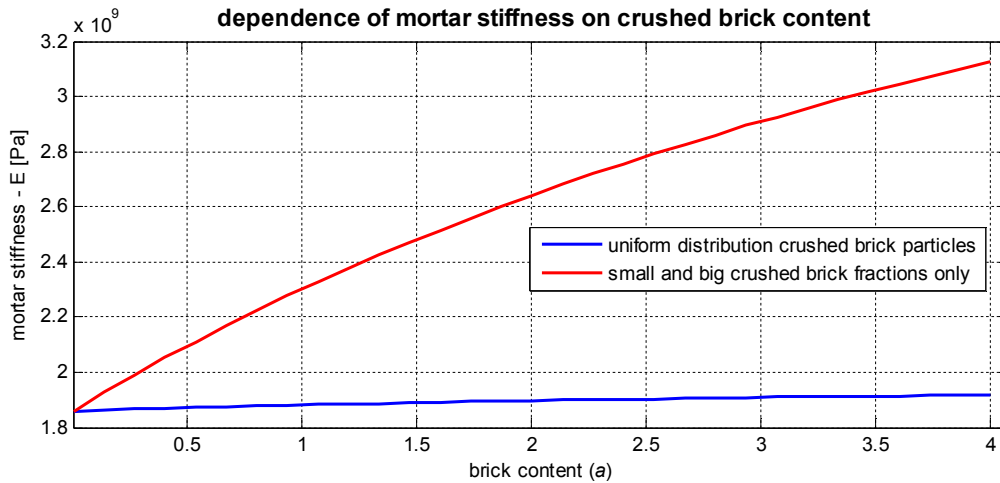


Fig. 9.7: Dependence of mortar stiffness on brick content

The increase of mortar effective stiffness is rather high. However, the increased effective stiffness is balanced by a quite significant reduction of the deviatoric stress within the matrix, ensuring the bigger mortar strength. The dependence of the deviatoric stress in the matrix on crushed brick content, for the original and modified size distribution of crushed brick particles distribution, can be seen in the following figure:

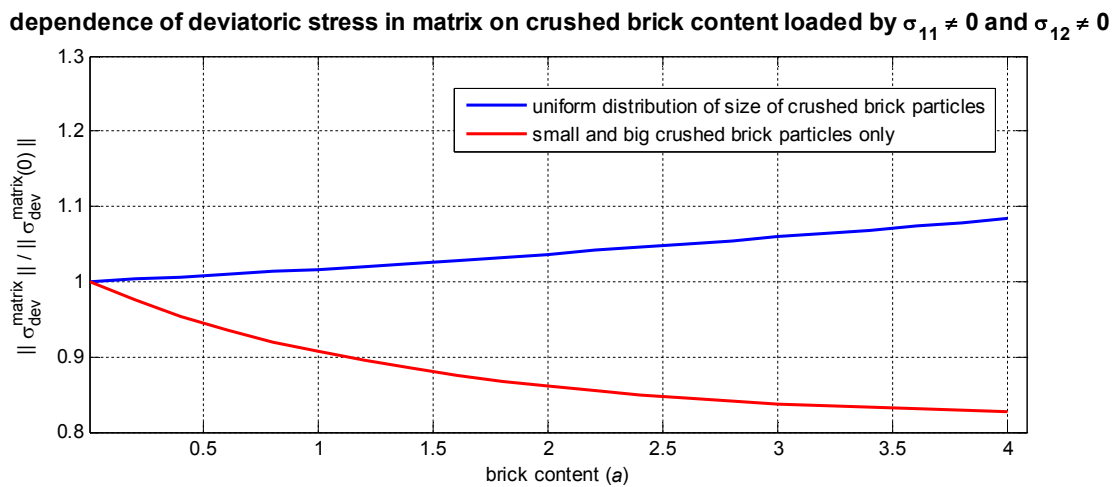


Fig. 9.7: Dependence of mortar stiffness on brick content

Conclusion

The assumption of C-S-H gel formation on the matrix-crushed brick interface has a major influence on behavior of the cocciopesto mortars. According to the calculations based on micromechanical approach, the C-S-H gel coating plays a significant role, especially in case of small crushed brick fractions.

The main factor influencing the behavior of the crushed bricks (or other clay products, such as tiles or pottery) in a mix is the coating thickness to brick fragments size ratio. With the increasing ratio, ensured by an addition of the small crushed brick fractions, the mortar becomes stiffer and the deviatoric stress in a lime matrix decreases. Since the lime matrix is considered as the weakest constituent, the reduction of the deviatoric stress should result in an increase of the mortar strength. It is assumed that mainly the deviatoric stress component is responsible for the failure of the material and therefore the stress deviator, J_2 , was chosen as an adequate indicator.

The proposed model also confirmed the negative effect of voids in lime mortars, since the increased porosity causes quite large increase of the deviatoric stress within the lime matrix and makes the mortar more compliant.

It was also found that the addition of crushed bricks, having a bigger diameter, should make the mortar more compliant and cause an increase of the deviatoric stress in the matrix. The addition of crushed bricks of a small size results in the opposite behavior – the mortar becomes stiffer and the deviatoric stress in the lime matrix is reduced.

However, the results provided in this work, cannot be considered as exact because of a few simplifications and uncertainties in the calculation. The Mori-Tanaka homogenization technique assumes the materials to behave linearly and it is expected that the C-S-H gel should have additional positive effect on the mortar strength, if the non-linear behavior were considered. The thickness of the C-S-H gel coating, 20 μm , cannot be taken as the exact universal value, since it is dependent on the chemical composition of the individual mortar constituents. There is also uncertainty around the reduction of porosity, if the C-S-H gel is formed.

Despite the above mentioned simplifications, the model should be able to correctly predict the trends and serve for the optimization of the mortar towards the desired properties.

References

- [1] PICHLER B., HELLMICH CH.: *Upscaling quasi-brittle strength of cement paste and mortar: A multi-scale engineering mechanics model*, Cement and Concrete Research, No. 41, 2011, pages 467-476
- [2] ROYLANCE D.: *Mechanical Properties of Materials*, 2008
- [3] JIRÁSEK M.: *Damage and Fracture in Geomaterials*, REGC, 2007, pages 879-892
- [4] GROSS D., SEELIG T.: *Fracture Mechanics with an Introduction to Micromechanics*, Springer, 2006
- [5] BÖHM H.J.: *A Short Introduction to Basic Aspects of Continuum Micromechanics*, ILSB Report 208, 2011
- [6] PALOMO A., VLANCO-VARELA M.T., MARTINEZ-RAMIREZ S., PUERTAS F., FORTES C.: *Historic Mortars: Characterization and Durability. New Tendencies for Research*
- [7] DELATTE N.J.: *Lessons from Roman Cement and Concrete*, Journal of Professional Issues in Engineering Education and Practice, July 2001, pages 109-115
- [8] MOROPOULOU A., BAKOLAS A., BISBIKOU K.: *Investigation of the technology of historic mortars*, Journal of Cultural Heritage, No. 1, 2000, pages 45-58
- [9] BARONIO G., BINDA L., LOMBARDINI N.: *The role of brick pebbles and dust in conglomerates based on hydrated lime and crushed bricks*, Construction and Building Materials, Vol. 11, No. 1, 1997, pages 33-40
- [10] BAKOLAS A., AGGELAKOPOULOU E., MOROPOULOU A.: *Evaluation of pozzolanic activity and physico-mechanical characteristics in ceramic powder-lime pastes*, Journal of thermal Analysis and Calorimetry, Vol. 92, 2008, No. 1, pages 345-351
- [11] MOROPOULOU A., CAKMAK A.S., LOHVYN N.: *Earthquake resistant construction techniques and materials on Byzantine monuments in Kiev*, Soil Dynamics and Earthquake Engineering, No. 19, 2000, pages 603-615
- [12] MOROPOULOU A., CAKMAK A.S., BISCONTIN G., BAKOLAS A., ZENDRI E.: *Advanced Byzantine cement based composites resisting earthquake stresses: the crushed brick / lime mortars of Justinian's Hagia Sophia*, Construction and Building Materials, No. 16, 2002, pages 543-552

- [13] ÇAKMAK A.S., MOROPOULOU A., MULLEN C.L.: *Interdisciplinary study of dynamic behavior and earthquake response of Hagia Sophia*, Soil Dynamics and Earthquake Engineering, No. 14, 1995, pages 124-133
- [14] GIAVARINI C., FERRETTI A.S., SANTARELLI M.L.: *Mechanical characteristics of Roman "opus caementicium"*, Fracture and Failure of Natural Building Stones, 2006, pages 107-120
- [15] SIDDALL R.: *Textures in Roman Lime Mortars using Polarising Light Microscopy*, <http://www.ucl.ac.uk/~ucfbrxs/PLMlimes.html>
- [16] LUO H.A., WENG G.J.: *On Eshelby's inclusion problem in a three-phase spherically concentric solid, and a modification of Mori-Tanaka's method*, Mechanics of Materials No. 6, 1987, pages 347-361
- [17] BÖKE H., AKKURT S., İPEKOĞLU B., UĞURLU E.: *Characteristics of brick used as aggregate in historic brick-lime mortars and plasters*, Cement and Concrete Research 36, 2006, pages 1115-1122
- [18] SELVAM P.R., SUBRAMANI V.J., MURRAY S., HALL K.: *Potential Application of Nanotechnology on Cement Based Materials*, 2009
- [19] CONSTANTINIDES G., ULM F.J.: *The effect of two types of C-S-H on the elasticity of cement-based materials: Results from nanoindentation and micromechanical modeling*, Cement and Concrete Research, Vol. 34, Issue 1, 2004, pages 67-80
- [20] JEFFREY J. T., HAMLIN M. J.: *A colloidal interpretation of chemical aging of the C-S-H gel and its effects on the properties of cement paste*, Cement and Concrete Research 36, 2006, pages 30- 38
- [21] MOROPOULOU A., BAKOLAS A., BISBIKOU K.: *Characterization of ancient, Byzantine and later historic mortars by thermal and X-ray diffraction techniques*, Thermochemica Acta, No. 269/270, 1995, pages 779-995
- [22] MOROPOULOU A., BAKOLAS A., ANAGNOSTOPOULOU S.: *Composite materials in composite structures*, Cement & Concrete Composites, No. 27, 2005, pages 295-300
- [23] HENDRICKX R. et. al.: *Observation of the failure mechanism of brick masonry doublets with cement and lime mortars by X-ray CT*, International Micro-CT symposium, Katholieke Universiteit Leuven, 2009 (report available at <https://lirias.kuleuven.be/bitstream/123456789/260821/1/Presentation+microCT+RH.pdf>)
- [24] DRDÁČKÝ M., MICHOINOVÁ D.: *Lime mortars with natural fibres*, in „Brittle Matrix Composites 7“ Proceedings of the 7th Int. Symposium (A.M.Brandt,

V.C.Li, I.H.Marshall,eds.), pages 523-532, 13-15 October, Warsaw, Woodhead Publishing Ltd./Zturek Research Sci.Inst., Cambridge and Warsaw, ISBN 1-85573-769-8, ISBN 83-917926-6-8, 2003

[25] Material Science publishing and information provision - AZoM.com, The A to Z of Materials: <http://www.azom.com/article.aspx?ArticleID=1114>

[26] VELOSA A.L., ROCHA F., VEIGA R.: *Influence of chemical and mineralogical composition of metakaolin on mortar characteristics*, Acta Geodyn. Geomater., Vol. 6, No. 1 (153), 2009, pages 121-126

[27] ŠMILAUER V., HLAVÁČEK P., ŠKVÁRA F., ŠULC R., KOPECKÝ L., NĚMEČEK J.: *Micromechanical multiscale model for alkali activation of fly ash and metakaolin*, Journal of Materials Science, 2011, pages 1-11